

การจำลองเซลล์เชื้อเพลิงชนิดเชื้อเพลิงผ่านอิเล็กโตรไลต์แบบพอลิเมอร์



นางสาว วรสร โพธิ์ทอง

สถาบันวิทยบริการ

จุฬาลงกรณ์มหาวิทยาลัย

วิทยานิพนธ์นี้เป็นส่วนหนึ่งของการศึกษาตามหลักสูตรปริญญาวิศวกรรมศาสตรมหาบัณฑิต

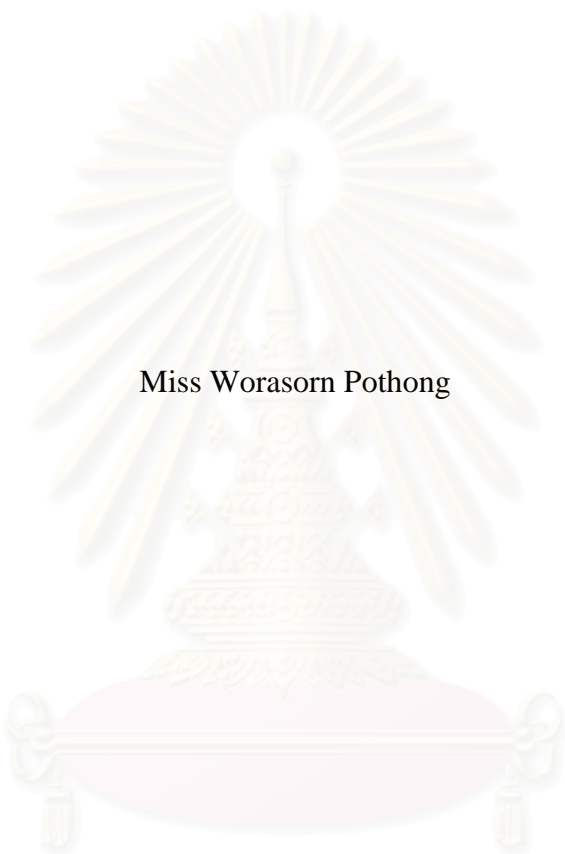
สาขาวิชาวิศวกรรมเคมี ภาควิชาวิศวกรรมเคมี

คณะวิศวกรรมศาสตร์ จุฬาลงกรณ์มหาวิทยาลัย

ปีการศึกษา 2550

ลิขสิทธิ์ของจุฬาลงกรณ์มหาวิทยาลัย

SIMULATION OF POLYMER ELECTROLYTE MEMBRANE FUEL CELLS



Miss Worasorn Pothong

สถาบันวิทยบริการ

A Thesis Submitted in Partial Fulfillment of the Requirements
for the Degree of Master of Engineering Program in Chemical Engineering

Department of Chemical Engineering

Faculty of Engineering


Chulalongkorn University

Academic Year 2007

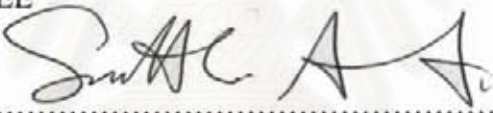
Copyright of Chulalongkorn University

Thesis Title SIMULATION OF POLYMER ELECTROLYTE MEMBRANE
FUEL CELLS
By Miss Worasorn Pothong
Field of Study Chemical Engineering
Thesis Advisor Assistant Professor Amornchai Arpornwichanop, D.Eng.

Accepted by the Faculty of Engineering, Chulalongkorn University in Partial
Fulfillment of the Requirements for the Master's Degree

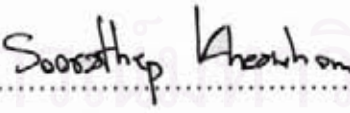

..... Dean of the Faculty of Engineering
(Associate Professor Boonsom Lerdhirunwong, Dr.Ing.)

THESIS COMMITTEE


..... Chairman
(Associate Professor Suttichai Assabumrungrat, Ph.D.)


..... Thesis Advisor
(Assistant Professor Amornchai Arpornwichanop, D.Eng.)


..... External Member
(Assistant Professor Worapon Kiatkittipong, D.Eng.)


..... Member
(Soorathep Kheawhom, Ph.D.)

วรสร โพธิ์ทอง : การจำลองเซลล์เชื้อเพลิงชนิดเยื่อเลือกผ่านอิเล็กโตรไลต์แบบพอลิเมอร์.
(SIMULATION OF POLYMER ELECTROLYTE MEMBRANE FUEL CELLS)
อ. ที่ปรึกษา : ผศ.ดร. อมรชัย อภรณ์วิชานพ, 69 หน้า.

งานวิจัยนี้มุ่งเน้นการวิเคราะห์สมรรถนะของเซลล์เชื้อเพลิงชนิดเยื่อเลือกผ่านอิเล็กโตรไลต์แบบพอลิเมอร์ แบบจำลองซึ่งพิจารณาสถานะของน้ำภายในเซลล์แบบ 2 เฟสถูกนำมาใช้เพื่อจำลองพฤติกรรมของเซลล์เชื้อเพลิงชนิดนี้ ที่สภาวะกึ่งตัวและอุณหภูมิคงที่ โดยทำการวิเคราะห์สมรรถนะของเซลล์เชื้อเพลิงโดยคำนึงถึงผลของความต้านทานการถ่ายโอนมวลของสารตั้งต้นที่เป็นผลมาจากการท่วมของน้ำภายในเซลล์ รวมถึงศึกษาอิทธิพลของตัวแปรดำเนินงานที่สำคัญ ได้แก่ อุณหภูมิ ความดัน และความชื้นของสารตั้งต้น โดยแสดงอยู่ในรูปของการกระจายตัวขององค์ประกอบของก๊าซ ค่ากระแสไฟฟ้าที่ได้ต่อพื้นที่ (current density) ค่าความต่างศักย์ของเซลล์ (cell voltage) และค่ากำลังไฟฟ้าที่ได้ต่อพื้นที่ (power density) ผลการศึกษาพบว่าสมรรถนะของเซลล์เชื้อเพลิงเพิ่มขึ้นเมื่ออุณหภูมิดำเนินการ ความชื้นของสารตั้งต้น และ ความดันมีค่าเพิ่มขึ้น ในทางกลับกัน สมรรถนะของเซลล์เชื้อเพลิงจะมีค่าลดลงเมื่ออุณหภูมิทางเข้าของเชื้อเพลิงและอากาศเพิ่มขึ้น เนื่องจากอุณหภูมิที่เพิ่มขึ้นทำให้เยื่อเลือกผ่านแห้ง (dehydration of membrane) นอกจากนี้ยังพบว่าปริมาณน้ำที่ท่วมเซลล์ เชื้อเพลิงเพิ่มขึ้นเมื่อดำเนินงานที่สภาวะความหนาแน่นกระแสสูง การเกิดน้ำท่วมเซลล์ส่งผลทำให้ สัดส่วนช่องว่าง (void fraction) ภายในขั้วแคโทดลดลง ทำให้ออกซิเจนแพร่ผ่านได้น้อยลง ส่งผลให้ค่าความสูญเสียศักย์ไฟฟ้าเนื่องจากความแตกต่างความเข้มข้นของสารตั้งต้นมีค่าสูงขึ้น

สถาบันวิทยบริการ
จุฬาลงกรณ์มหาวิทยาลัย

ภาควิชา.....วิศวกรรมเคมี.....
สาขาวิชา.....วิศวกรรมเคมี.....
ปีการศึกษา.....2550.....

ลายมือชื่อนิสิต..... ๑๕๕๖ โปธิ์ทอง.....
ลายมือชื่ออาจารย์ที่ปรึกษา..... ออมรชัย อภรณ์วิชานพ.....

4970551921 : MAJOR CHEMICAL ENGINEERING

KEY WORD : POLYMER ELECTROLYTE MEMBRANE FUEL CELL/
MATHEMATICAL MODEL / SIMULATION / PERFORMANCE ANALYSIS

WORASORN POTHONG : SIMULATION OF POLYMER ELECTROLYTE
MEMBRANE FUEL CELLS. THESIS ADVISOR: ASSISTANT PROFESSOR
AMORNCHAI ARPORNWICHANOP, D.Eng., 69 pp.

This research concentrates on the performance analysis of a polymer electrolyte membrane fuel cell (PEMFC). A two-phase model taken into account the formation of liquid water is used to simulate the steady state behavior of the PEMFC under isothermal condition. The mass transfer resistance of reactants due to a water flooding effect is taken into account to analyze cell performance. The effect of key operating conditions such as temperature, pressure and humidification of reactant gases on the PEMFC in terms of the distribution of gas composition and current density, and cell voltage and power density is studied. Simulation studies show that the performance of PEMFC increases when operating temperatures, the humidity of the fuel gas and air gas, and operating pressure are increased. In contrast, the cell performance decreases while the anode and cathode inlet temperatures increase due to the dehydration of membrane. The water flooding at the cathode side increases with increasing operating current density. The occurrence of water flooding results in lower void fraction in the cathode and thus, less oxygen can diffuse to the catalyst layer. Therefore, higher concentration loss is observed.

สถาบันวิทยบริการ
จุฬาลงกรณ์มหาวิทยาลัย

Department.....Chemical Engineering...

Field of study...Chemical Engineering...

Academic year.....2007.....

Student's signature...*Worasorn Pothong*.....

Advisor's signature...*Amornchai Arpornwichanop*.....

ACKNOWLEDGEMENTS

I would like to thank and express my sincere gratitude to my advisor, Assistant Professor Amornchai Arpornwichanop, for his supervision, encouraging guidance, advice, discussion and helpful suggestions throughout the course of this Master Degree study. It has been a great opportunity and experience for me to work with him. Furthermore, I am also grateful to Associate Professor Suttichai Assabumrungrat, Assistant Professor Worapon kiatkittipong and Dr. Soorathep Kheawhom for serving as the chairman and member of thesis committee, respectively.

Financial supports from the Thailand Research Fund (TRF-Master Research Grants) and the Energy Research Institute and the Graduate School of Chulalongkorn University are gratefully acknowledged.

I would also like to thank all members of Control and Systems Engineering Research Center for their friendship and support over the years.

I owe special thanks to Mr. Wongsakorn Chantrapornsyl for his suggestions, support, encouragement and all of the good things that he has given to me.

Most of all, I would like to express the highest gratitude to my family for their love, inspiration, encouragement and financial support throughout this study.

สถาบันวิทยบริการ
จุฬาลงกรณ์มหาวิทยาลัย

CONTENTS

	PAGE
ABSTRACT IN THAI	iv
ABSTRACT IN ENGLISH	v
ACKNOWLEDGEMENTS	vi
CONTENTS	vii
LIST OF TABLES	x
LIST OF FIGURES	xi
NOMENCLATURES	xiv
 CHAPTER	
I INTRODUCTION	1
1.1 Research Objectives	3
1.2 Scopes of Research	3
1.3 Thesis outline	3
II LITERATURE REVIEWS	4
2.1 Modeling of PEMFC.....	4
2.1.1 Electrochemical model.....	4
2.1.2 Transportation model.....	7
2.2 Water management in PEMFC	8
III THEORY	11
3.1 Fuel cell.....	11
3.1.1 Cell Component	12

CHAPTER	PAGE
3.1.2 Advantages of fuel cell	13
3.2 PEM Fuel Cell.....	13
3.2.1 Physical structure of PEM	13
3.2.2 Design, component materials, and assembly	14
3.2.3 Operation principle of PEM.....	16
IV MATHEMATICAL MODEL OF PEMFC	18
4.1 Mass balances	18
4.2 Theoretical fuel cell potential	21
4.3 Voltage Losses	22
4.3.1 Activation Polarization	22
4.3.2 Ohmic Losses.....	24
4.3.3 Concentration Polarization.....	25
4.3.4 The Actual Voltage of Fuel Cell.....	27
4.4 Power Generation.....	28
4.5 Efficiency of Cell	29
V SIMULATION RESULTS AND DISCUSSION.....	30
5.1 Model validation	30
5.2 Performance of PEMFC at standard condition	33
5.3 Effect of operating temperature	37
5.4 Effect of gas humidity	43
5.5 Effect of anode inlet temperature.....	54
5.6 Effect of cathode inlet temperature.....	56

CHAPTER	PAGE
5.7 Effect of operating pressure	57
5.8 Effect of water flooding	59
VI CONCLUSION AND RECOMMENDATIONS.....	62
5.1 Conclusions	62
5.2 Recommendations	63
REFERENCES.....	64
APPENDICX.....	67
Appendix A	68
VITA	69



สถาบันวิทยบริการ
จุฬาลงกรณ์มหาวิทยาลัย

LIST OF TABLES

	PAGE
Table 3.1 Fuel cell type attributes	12
Table 3.2 The development of proton conductive membranes	15
Table 5.1 Model parameters used in the simulation.....	31
Table 5.2 Operation conditions of PEMFC at the standard condition	33



สถาบันวิทยบริการ
จุฬาลงกรณ์มหาวิทยาลัย

LIST OF FIGURES

		PAGE
Figure 3.1	A schematic diagram of a polymer electrolyte membrane (Lee et al., 1998)	13
Figure 3.2	Basic structure and composition of some perfluorosulfonic acid membrane of DuPont, Dow, and Asahi Chemical	16
Figure 3.3	Flow diagram of polymer electrolyte fuel cell.....	17
Figure 4.1	Schematic diagram of PEM fuel cell.....	19
Figure 4.2	I-V curve of a polymer electrolyte membrane fuel cell	28
Figure 5.1	Comparison between model prediction and experimental data (Liu et al., 2005).....	32
Figure 5.2	Comparison between a single-phase and two-phase PEMFC model.....	32
Figure 5.3	Profiles along the cell channel: (a) Current density, (b) hydrogen mole fraction at the anode, (c) oxygen mole fraction at the cathode, (d) water mole fraction at the anode, (e) water mole fraction at the cathode, and (f) Membrane Conductivity	34
Figure 5.4	Profiles along the cell channel: (a) Current density, (b) Anode hydrogen mole fraction, (c) Cathode oxygen mole fraction, (d) Anode water mole fraction, (e) Cathode water mole fraction, and (f) Membrane Conductivity.....	38
Figure 5.5	Effects of operating temperature at different current density on (a) cell voltage and (b) power density.	42

Figure 5.6	Distribution of current density along the cell channel at different gas inlet humidity at (a) anode channel and (b) cathode channel	44
Figure 5.7	Distribution of hydrogen along the cell channel at different gas inlet humidity at (a) anode channel and (b) cathode channel.....	45
Figure 5.8	Distribution of oxygen along the cell channel at different gas inlet humidity at (a) anode channel and (b) cathode channel.....	46
Figure 5.9	Distribution of anode vapor water along the cell channel at different gas inlet humidity at (a) anode channel and (b) cathode channel	47
Figure 5.10	Distribution of cathode vapor water along the cell channel at different gas inlet humidity at (a) anode channel and (b) cathode channel.	48
Figure 5.11	Distribution of membrane conductivity along the cell channel at different gas inlet humidity at (a) anode channel and (b) cathode channel.	49
Figure 5.12	Distribution of membrane resistance along the cell channel at different gas inlet humidity at (a) anode channel and (b) cathode channel.	50
Figure 5.13	Distribution of concentration loss along the cell channel at different gas inlet humidity at (a) anode channel and (b) cathode channel.	51

Figure 5.14	Effects of gas inlet humidity at different current density on cell voltage: (a) change of anode relative humidity, and (b) changing of cathode relative humidity.	52
Figure 5.15	Effects of gas inlet humidity at different current density on cell power density: (a) change of anode relative humidity, and (b) changing of cathode relative humidity	53
Figure 5.16	Effect of anode inlet temperature at different current density on (a) cell voltage and (b) power density.	55
Figure 5.17	Effect of cathode inlet temperature at different current density on (a) cell voltage and (b) power density.....	56
Figure 5.18	Effect of operating pressure at different current density on (a) cell voltage and (b) power density.....	58
Figure 5.19	Effect of current density on cell voltage and fraction of water flooding.	59
Figure 5.20	Effect of current density on cell voltage and fraction of water flooding at (a) $T = 353 \text{ K}$ and $P = 3 \text{ atm}$ and (b) $T = 363 \text{ K}$ and $P = 1 \text{ atm}$	60

NOMENCLATURES

- A = Electrode active area, cm^2
- a = The activity of water
- C_B = Bulk concentration of reactant (mol/m^3)
- $C_{i,a}$ = Concentration of reactant at air channel (mol/m^3)
- $C_{i,f}$ = Concentration of reactant at fuel channel (mol/m^3)
- $C_{p,f}, C_{p,a}, C_{p,mem}$ = Specific heat capacity of the gas streams and membrane (kJ/kg K)
- C_{O_2} = The concentration of oxygen (mol/m^3)
- C_S = Concentration of reactant at the surface of the catalyst (mol/m^3)
- D^{eff} = The effective diffusivity
- D_{ij} = The binary gas diffusion coefficient
- D_{O_2} = The diffusivity of oxygen (m^2/s)
- D_w = The water diffusivity through the membrane (mol/m s)
- $d_{h,a}, d_{h,f}$ = The channel hydraulic diameter
- E = Potential (Volt)
- E_0 = The cell potential (Volt)
- E_{thermo} = Thermodynamically predicted voltage of fuel cell (Volt)
- F = The Faraday constant (96485 C/mol)

- f_{pt} = Weight fraction of platinum on carbon
- f_{mem} = Weight fraction of ionomer
- G_0 = Gibbs free energy at the standard temperature and pressure
(25 °C and 1 atm)
- H_i = The enthalpy of mixture gases (J/s)
- h_a = Air channel height (m)
- h_f = Fuel channel height (m)
- i = Current density (A/ m²)
- i_0 = Exchange current density (A/ m²)
- i_L = The limiting current density (A/ m²)
- K_{mem} = The conductivity of membrane (S/m)
- $k_{a,mem}$ = Air channel heat transfer coefficient (kJ/ m² s K)
- $k_{f,mem}$ = Fuel channel heat transfer coefficient (kJ/ m² s K)
- k_a, k_f, k_{mem} = Thermal conductivity of gas streams and membrane (kJ/ m² s K)
- k_c = the condensation rate constant (s⁻¹)
- k_v = the evaporation rate constant (s⁻¹atm⁻¹)
- M = Molecular weight (kg/ kmol)
- m_i = The mass flow rate
- m_{pt} = Platinum loading inside the catalyst layer (kg Pt/ m²)

N	=	Flux of reactants (mol/s)
Nu	=	Nusselt number
N_w	=	The water vapor flux transport across the MEA
n	=	Number of electrons per molecule of $H_2 = 2$ electrons per molecule
n_d	=	The electro-osmotic drag coefficient
P	=	H_2 , O_2 and water partial pressures (atm)
P^{sat}	=	The saturation water pressure (atm)
P_0	=	Reference or standard pressure (1 atm)
P_c	=	The critical pressure (atm)
P_D	=	Power density (W/m^2)
p_w	=	Partial pressure of water vapor (atm)
Q	=	Heat flux out of fuel cell
q	=	Charge (Coulombs mol^{-1})
R	=	Universal gas constant (8.314 J/mol K)
R_i	=	Total cell internal resistance (Ω , ohm)
R_x	=	Reaction rate ($mol/ s m^2$)
RH	=	Relative Humidity
r_{gg}	=	radius of liquid water (m)
S_w	=	The interfacial transfer of water between liquid and water vapor

s = The liquid saturation level which is the fraction of void volume occupied by liquid water

T_{mem} = Temperature of the cell (K)

T_a, T_f = Temperature at air and fuel channel (K)

T_c = The critical temperature (K)

u_a = Fuel velocity at fuel channel (m/s)

u_f = Fuel velocity at fuel channel (m/s)

V = Operating voltage of fuel cell (Volt)

v_{mem} = Volume of ionomer (m³)

v_{total} = Volume of solid and void (m³)

X_w = The molar fraction of water

W = Channel width (m)

W_{el} = Electrical work (J mol⁻¹)

w_c, w_{pt}, w_{mem} = Mass of carbon, platinum, and membrane (kg)

GREEK LETTERS

α = The transfer coefficient (Tafel slope)

ΔG = Gibbs free energy

ΔH = Hydrogen's heating value

$(-\Delta H_{rxn})$ = Enthalpy charge of reaction (kJ/ mol)

- δ = Total Membrane and electrode thickness (m)
- δ_{solid} = Membrane and electrode thickness using in two-phase model (m)
- δ_{w_mem} = Water flooding thickness in membrane using in two-phase model (m)
- λ = Water content in membrane
- ε = The porosity of electrode
- η_{act} = Activation losses due to reaction kinetics (Volt)
- η_{eff} = The cell efficiency
- η_{conc} = Concentration losses due to mass transport (Volt)
- η_{ohmic} = Ohmic losses from ionic and electronic resistance (Volt)
- ρ = Specific resistance of membrane (Ω m)
- $\rho_a, \rho_f, \rho_{mem}$ = Density of gas streams and membrane (kg/m^3)
- ρ_w = Density of water (kg/m^3)

SUBSCRIPTS

- a = Anode side of cell
- c = Cathode side of cell

CHAPTER I

INTRODUCTION

Fuel cell technology has been developed very fast recently as it is possible to replace internal engine and supplemental power generators. Among the various types of fuel cells, the polymer electrolyte membrane fuel cell (PEMFC) emerges as an interesting technology, especially for portable power supply units. It operates at low temperatures and offers low weight and volume, and high power density.

PEMFC is characterized by the use of a perfluorosulfonic membrane as the electrolyte. This type of membrane shows a good proton conductor. That is, in the presence of water, the sulfonic groups easily dissociate into SO_3^- (fixed charge) and H^+ (mobile charge) and thus, the protons encounter a low resistance in moving across the membrane. In PEMFC, the membrane accomplishes both the functions of H^+ transfer from anode to cathode and the reactant separation. For PEMFC operation, hydrogen is used as fuel. The electrodes are formed by a porous gas diffusion layer and a porous catalytic layer containing a noble catalyst (Pt) (Costamagna, 2001).

It is well known that commercial polymer electrolyte membrane being currently used in PEMFCs should be well-hydrated to maintain high proton conductivity. Generally, water management is critical in PEMFC performances as excessive liquid water can cause flooding of the pores in electrode thus causing higher mass transfer resistance of reactants. This is especially true on the cathode side where water is produced from electrochemical reaction. In addition, some water is transferred from the anode to the cathode due to electro-osmosis. The balance of water is more complicated due to the fact that water content in the membrane and liquid water distribution in the electrode are not uniform.

Mathematical modeling of fuel cells has become more and more important over the recent years in order to study the behavior of the fuel cell integrated in a power system. In general, basic fuel cell models require an accurate current density-

voltage curve, which refers to as the electrical characteristics of PEMFC. This is a key feature to predict a cell performance. The performance of fuel cells is known to be influenced by operating conditions. Busquet et al. (2004) studied the effects of stack temperatures and oxygen partial pressure on the performance of PEMFC. Lee and Chu (2006) carried out the simulation of the conventional flow field of PEMFC using a steady state isothermal model under various humidity conditions at the cathode side.

Although water transport phenomena has a significant influence on performance of PEMFC, there is a limited number of researches focusing on the water management within PEMFC. For examples, Baschuk and Li (2000) studied the effect of water flooding in the PEM fuel cells. The effect of the variation in the degree of water flooding on the cell performance was also investigated. Ramousse et al. (2005) proposed a fuel cell model that takes into account gas diffusion in the porous electrodes, water diffusion and electro-osmotic transport through the polymeric membrane, and heat transfer in both the Membrane Electrodes Assembly (MEA) and bipolar plates. Their results showed that the feeding gas temperature has an effect on the cell temperature. Clearly, the cell performance and water management issues are closely related; the cell performance is significantly influenced by thermal management.

In this work, we focus on the study of the steady-state behavior of PEMFC with respect to the effect of changing operating conditions such as temperature, pressure, humidification of the reactant gases and porosity of electrode. Mathematical model of PEMFC based on a two-phase model under isothermal operation is employed for such a purpose. The mass transfer resistance of reactants due to water flooding is taken into account to analyze cell performance. The simulation results of the two-phase model are compared with that of a single-phase model in which water flooding is not considered.

1.1 Research objective

The objective of this study is to investigate the performance of a polymer electrolyte membrane fuel cell (PEMFC) under isothermal and steady state conditions by considering the effect of operating condition and liquid water formation.

1.2 Scopes of research

In this study, an analysis of a polymer electrolyte membrane fuel cell (PEMFC) under isothermal and steady state conditions is performed via simulation studies using Matlab program. The model of PEMFC is based on a two-phase model consisting of mass balance and detailed electrochemical models. The mass balance is used to describe the distribution of reactants and reaction product along the flow direction at fuel and air channels whereas the electrochemical model taken all various voltage losses in account is employed for explaining the electrical characteristics of fuel cell. In addition, the formation of liquid water and its effect on the cell performance is considered. Based on the developed model of PEMFC, the effect of operating parameters, i.e., operating temperature and pressure and gas humidity, on cell performance is analyzed.

1.3 Thesis outline

This thesis is organized as follows. First, in Chapter II, the literature reviews related to the basic principle of fuel cell and polymer electrolyte membrane fuel cell (PEMFC) and the modeling of PEMFC are presented. Next, the theory of fuel cells and basic operation of PEMFC are presented in Chapter III, The mathematical model of PEMFC based on mass balance and electrochemical equations are explained in Chapter IV. Then, the simulation results are presented in Chapter V. Finally, the conclusions and the recommendations for future work are given in Chapter VI.

CHAPTER II

LITERATURE REVIEWS

Among the different types of fuel cell, polymer electrolyte membrane (PEM) fuel cells have been received most attention due to its simplicity, viability, and quick start-up. To improve the performance of PEMFC, there are still challenging problems needed to be solved, for examples, finding alternative low-cost materials, developing manufacturing techniques for cell components, and managing water and heat in the cells. To address these issues, modeling investigations are powerful and affordable alternative to experimental studies. A number of fuel cell models have been proposed in the literature over the last two decades. In this chapter, literature reviews related to the model development of a proton exchange membrane fuel cell (PEMFC) are provided.

2.1 Modeling of PEMFC

Mathematical models of PEMFCs proposed during the early years were typically based on one-dimensional and steady-state model accounting for mass transport and electrochemical phenomena. The developed models have been applied for a variety of purposes such as prediction of the typical electrical characteristics (current-potential) of cell, parametric analysis, and investigation of gas composition, temperature, and pressure distribution within fuel cell stack.

2.1.1 Electrochemical model

The electrochemical model is used to characterize the electrical characteristics of a cell. It demonstrates the relationship between operating cell voltage and current density. In addition, the model is useful in determining kinetic parameters and general ohmic resistance from experimental data. It is noted that the development of fuel cell models generally require accurate electrochemical model. In the past years, a number of researches have been carried out to develop the electrochemical model for

predicting the actual operating cell voltage as a function of current density. In addition, some researchers investigated the PEMFC performance based on the electrochemical model.

Wang et al. (2003) studied the effects of different operating parameters such as operating temperatures, cathode and anode humidification temperatures, and operating pressures, on the performance of proton exchange membrane (PEM) fuel cell by using pure hydrogen on the anode side and air on the cathode side. The results were demonstrated by polarization curves, and agreed well with experimental data.

Busquet et al. (2004) studied the effects of stack temperature and the oxygen partial pressure on the performance of PEMFC. The developed model of fuel cell was used to analysis a polarization curves. The operating condition of fuel cell was chosen to avoid the limitation of mass transfer process.

Chen et al. (2006) presented a simple electrochemical model that can be used for optimization of a fuel cell. The fuel cell's design parameters are chosen so as to globally minimize its total annualized cost for a given power production level.

The effect of several critical operating conditions on the performance of an 8-cell stack are studied by Santa Rosaa et al. (2007) based on varying operating conditions such as cell temperature, air flow rate, and hydrogen pressure and flow rate. They proposed that although improving the electrochemical reactions kinetics and decreasing the polarization effects, the increasing of the stack temperature leads to membrane excessive dehydration (loss of sorbet water) and the increasing of the stack ohmic resistance (lower performance).

Santarelli et al. (2006) discussed a procedure of parameter estimation applied to the evaluation of some operating parameters of PEMFC. A parametric analysis of the PEMFC fed with pure hydrogen and air and operated at temperatures in the range of 50 °C to 80°C was done and the results showed that three parameters of the cell polarization model can be simultaneously estimated: the cathode exchange current density, the cell resistance and the internal current density.

Amirinejad et al. (2006) studied experimentally the effect of external humidity on fuel cell performance under various temperature and pressure conditions using dry and humidified hydrogen and oxygen as the fuel and reactant gases, respectively.

Lee and Chu (2006) investigated the location of the gas–liquid interface under various humidity conditions in the cathode gas diffusion layer and the conventional flow field of PEMFC based on steady state isothermal model. These works showed the humidity related with membrane resistant.

Tsai et al. (2006) simulated the transport phenomena of oxygen in cathode gas diffusion layer (GDL) of PEMFC. It was found that the concentration flux of oxygen across the GDL was primarily dominated by the thickness and porosity of GDL. For a thicker GDL, the diffusion resistance increased and thus lowered the cell performance especially under high current density condition. On the other hand, an increase of porosity enhanced the transport of oxygen and resulted in significant improvement of cell performance. The influences of system parameters including the temperature, channel height, inlet velocity, and inlet pressure on the diffusion of oxygen in GDL were also examined systematically.

Katsaounis et al. (2006) discussed the conductivity of fully hydrated Nafion membranes on the performance of fuel cells. It was shown that the Nafion conductivity contains two components: one constant corresponding to proton transport in the aqueous phase of the membrane and the other exponentially dependent on potential, linearly increasing with membrane thickness and strongly increasing with hydrogen partial pressure at the anode. A simple mathematical model was developed and shown to provide a semi quantitative fit to the experimental I–V curves.

In addition, Carnes and Djilali (2005) proposed the parameter estimation for the development of mathematical models for polymer electrolyte membrane fuel cells (PEMFCs). The estimate parameters in a 1-D PEMFC model included effective membrane conductivity, exchange current densities, and oxygen diffusion coefficients.

2.1.2 Transportation model

As electrochemical models lack the fundamental description of detailed inner-cell operating conditions. Reactant gases, temperature, current density, etc. vary along the flow. These are critical for accurate prediction of cell performance. In general, the transport and electrochemical processes occur throughout the flow direction and various cell layers.

Liu et al. (2006) indicated that the temperature gradient inside the fuel cell stack was determined by the flow rate of the cooling air, especially, if the air flow rate was too low, the stack could not be effectively cooled and the temperature will rise to a range that might cause unstable stack operation.

Brett et al. (2007) presented localized membrane resistance and current density distribution under the conditions of high air flow rate. The increasing of current is observed along the channel which is not predicted by the electrochemical model. This phenomenon is attributed to drying of the electrolyte at the start of the channel and is more pronounced with increasing operating temperature. These works showed that the study of temperature, reactant flow rates, and pressures is not enough to predict fuel cell performance.

Shimpalee et al. (1999) studied the effects of humidity. Experimental results showed that inlet gas humidity has a significant influence on the performance of a PEMFC. They indicated that the ionic resistance of the electrolyte membrane depended on the activity of water at the membrane surface. Water flux and activities change along the flow field direction. Detailed velocity fields, pressure profiles, and current density distributions are obtained and predictions from the full-cell model are compared with the experimental data.

Jeng et al. (2004) studied a two-dimensional model involving kinetics and mass transfer in a PEM fuel cell cathode. The oxygen mass transfer in the gas diffusion layer (GDL) was described using a pure diffusion equation that introduced equivalent oxygen diffusivity. The results showed that the GDL effectiveness decreased with the cell current density and increased with the width of the gas flow channels. The PEM fuel cell performance decreased with an increase in GDL

thickness if the GDL porosity is low. However, when a high-porosity GDL was used, the optimal thickness became an indicator determining the maximal PEM fuel cell performance.

2.2 Water management in PEMFC

Water management is the most important factor involving the performance of PEMFC. A careful water management is necessary to ensure that the membrane remain fully hydrated in order to improve the ionic conductivity and to avoid electrode flooding. In general, during fuel cell operation, humidification is applied to the inlet gases of the anode and cathode in order to supply water to the membrane region. If the water generated is not removed from the cathode at a sufficient rate, cathode flooding may result a decreased oxygen mass transfer.

Modeling of the water transport and distribution in PEMFC is a major issue in recent years. There are a number of investigations that analyze the effect of different operating condition on the water balance in PEMFC. Although different models have been proposed in the past year, they are valid only in the absence of liquid water; water condensation and evaporation phase change are not taken into account.

Recently, Wang et al. (2001) studied the two-phase flow and transport of reactants and products at the cathode side of PEMFC and classified the single and two phase regimes of water distribution and transportation by a threshold current density corresponding to liquid water at the membrane and electrode interface. When the cell is operated above the threshold current density, liquid water appears and a two phase zone forms within the porous cathode.

Liu et al. (2005) considered the water flooding and two-phase flow of reactants and products in cathode flow channels. The effects of flow field, cell temperature, and cathode gas flow rate and operation time on water build-up and cell performance were studied, respectively. Their results indicated that the liquid water accumulating in the cathode flow channels can reduce the effective electrochemical reaction area; it makes mass transfer limitation resulting in the cell performance loss. The water in flow channels at high temperature is much less than that at low

temperature. When the water flooding appears, increasing cathode flow rate can remove excess water and lead to good cell performance.

Mosdale et al. (1995) studied water and thermal management in order to explain the mass transport limitation in a fuel cell when operating with air as a cathode reactant. Their study concentrated on the modification of the structure of the electrode to increase the diffusion of oxygen that leads to a significant enhancement of the cell performance.

A transport phenomenon in a proton exchange membrane fuel cell (PEMFC) was simulated by Singh et al. (1999) to improve heat and water management. The model takes into account the diffusion of the humidified fuel and oxidant gases through the porous electrodes, and the convective and electro-osmotic transport of liquid water in the electrodes and the membrane. The results indicate that the cathode potential loss, associated with the slow O_2 reaction rate, is dominant at all practical current densities. The simulations showed a significant effect of water management on fuel cell performance.

Later, Baschuk and Li (2000) studied the effect of water flooding in the PEM fuel cells and stated that water management was one of the critical issues to be resolved in the design and operation of PEM fuel cells. The model was formulated for investigating the performance and operation of a single PEM fuel cell. A special feature of the model was that it included the effect of degree of water flooding in the cathode catalyst layer and cathode electrode backing region on the cell performance. The model predictions were compared with the existing experimental results available in the literature and excellent agreement of the cell polarization curves were observed.

Um and Wang (2005) developed a unified water transport equation for PEMFC, and showed that the effects of the flow arrangement, membrane thickness, and inlet gas humidity are important to determine fuel cell performance. Various modes of water transport, i.e., diffusion, convection and electro-osmotic drag, were incorporated in the unified water transport equation. An internal circulation of water with the aid of counter-flow design was found to be of vital importance for low-humidity operation. The effects of the flow arrangement, membrane thickness, and

inlet gas humidity as important determinants of fuel cell performance were also analyzed to elucidate fuel cell water transport characteristics.

Chang et al. (2006) investigated the characteristics of transport phenomena in the cathode gas diffusion layer (GDL) of a PEMFC and their influence on cell performance by utilizing a two-phase flow model. Their results showed that the liquid water generated by the electrochemical reaction could significantly reduce the effective porosity of the GDL under high current density conditions.

The importance of liquid water transport to the accurate modeling of fuel cell performance including the transport of liquid water within the PEMFC porous electrodes was studied by Siegel et al. (2004). Modeling results were presented that illustrated the importance of the transport of water within the porous sections of the cell and in the polymer regions of the MEA. The PEMFC was run, under standard conditions, at a cell temperature of 80 °C and a relative humidity of 100%. As current density is increased, the water content decreased as the anode dehydrated and the cathode water content increased. The results indicated that the total amount of water contained in the MEA decreased. This occurred because the vapor activity of the anode stream had dropped due to water vapor removal through MEA. This indicated that water transport by electro-osmotic drag was responsible for a significant fraction of the liquid water buildup and mass transfer of oxygen at the cathode.

In addition, Shah et al. (2006) presented several results pertaining to the effects of water on the current density (or cell voltage), demonstrating the role of micro-structure, liquid water removal from the channel, water activity, membrane and gas diffusion layer thickness and channel temperature at PEMFC cathode side. They investigated the polarization curves for several values of water activity in the channels. At fully humidified conditions, the effect of flooding is more pronounced at low cell voltages. The best performance of fuel cell is found at water activity = 1.

CHAPTER III

THEORY

This chapter presents general basic concepts of fuel cells (Section 3.1) such as basic principles, cell component and advantages. Section 3.2 presents detail of Polymer Electrolyte Membrane fuel cell (PEMFC) which is the fuel cell type of interest in this thesis.

3.1 Fuel cell

A fuel cell is an energy-conversion device that converts the chemical energy of fuel directly into DC electricity. Typically, a process of electricity generation from fuels involves several energy conversion steps:

- Combustion of fuel converts chemical energy of fuel into heat.
- This heat is then used to boil water and generate steam.
- Steam is used to run a turbine in a process that converts thermal energy into mechanical.
- And finally, mechanical energy is used to run a generator that generates electricity.

A fuel cell circumvents all these processes and generates electricity in single step without involving any moving parts. Such a device is simpler, thus less expensive and far more efficient than the four-step process previously depicted. A fuel cell is in some aspects similar to a battery. It has an electrolyte, and negative and positive electrode; and it generates DC electricity through electrochemical reactions. However, unlike a battery, a fuel cell requires a constant supply of fuel and oxidant. Also the electrodes in fuel cell do not undergo chemical changes. A fuel cell cannot be discharged as long as the reactants, fuel and oxidant, are supplied. Typical reactants

for fuel cells are hydrogen and oxygen; however, neither has to be in its pure form. Hydrogen may be present either in a mixture with other gases (such as CO_2 , N_2 , CO), or in hydrocarbons such as nature gas, CH_4 , or even in liquid hydrocarbons such as methanol, CH_3OH . Ambient air contains enough oxygen to be used in fuel cells. A fuel cell generates by-products; waste heat and water, and the system is required to manage those. Types of fuel cells are classified by electrolyte materials which are significantly related to operating temperature. Table 3.1 shows general information of different types of fuel cells.

Table 3.1 Fuel cell type attributes

	PEMFC	AFC	PAFC	MCFC	SOFC
Temperature ($^{\circ}\text{C}$)	60–120	120–225	150–220	600–700	650–1000
Electro-catalyst	Pt	Pt	Pt	Ni	Co–ZrO ₂ or Ni–ZrO ₂
Ionic-charge carrier	H ⁺	OH ⁻	H ⁺	CO ₃ ²⁻	O ²⁻
Membrane material	Nafion	Ni, Ag metal oxide	Silicon carbide	Lithium aluminate	Zirconia

3.1.1 Cell Component

Fuel cells consist of an electrolyte sandwiched between two electrodes (an anode and a cathode) where the electrochemical reactions take place. For hydrogen fuel and oxygen oxidant, the electrochemical combustion reaction consists of the oxidation of hydrogen at the anode and the reduction of oxygen at the cathode. The overall reaction yields water as the reaction product. In the operation of fuel cell, fuel (typically hydrogen) is fed to the anode where it is oxidized and electrons are released to the external (outer) circuit. Oxidant (typically oxygen) is fed to the cathode where it is reduced and electrons are accepted from the external circuit. The electron flow

(from the anode to the cathode) through the external circuit produces direct-current (DC) electricity.

3.1.2 Advantages of fuel cell

Fuel cells are a very promising energy technology with a myriad of possible applications. Fuel cells have many properties that make them attractive when compared with the existing, conventional energy conversion technologies. The advantages of fuel cell include high efficiency, low or zero emissions, Simplicity and promise of low cost and long life.

3.2 PEM fuel cell

3.2.1 Physical structure

A PEM fuel cell consists of two electrodes with a thin layer of catalyst in contact with a polymer membrane separating gas supply chambers. Hydrogen gas (H_2) which acts as fuel, is fed through a narrow channel from one end of the plate (Anode). Similarly, oxygen (O_2) enters the fuel cell from the other end of the plate (Cathode). Figure 3.1 presents a schematic diagram of a polymer electrolyte membrane fuel cell.

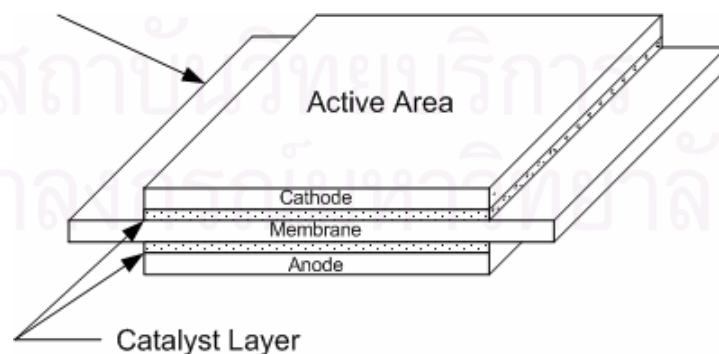


Figure 3.1 A schematic diagram of a polymer electrolyte membrane fuel cell

(Lee et al., 1998)

3.2.2 Design, component materials, and assembly

A basic design of single cell component involves the porous gas diffusion electrodes for the anode and cathode, the proton conducting membrane electrolyte, and the current collectors with the flow fields. The active layer with the electrocatalyst is generally deposited on the electrode but can also be deposited on the proton conducting membrane. In the former case, the electrode consists of three layers – a substrate layer (Teflonized carbon cloth or paper – about 30% Teflon), a diffusion layer (with high surface area carbon and Teflon, again about 30% Teflon), and the active layer with the nano-size Pt or Pt alloy particles, 200 to 400 nm, supported on high surface area carbon, e.g., Vulcan XC72. The active layers of the electrode are impregnated with the proton conductor (Nafion) to enhance the ionic conductivity in the three-dimensional reaction zone. The electrodes are hot-pressed on to the Nafion membrane at a temperature of about 130°C and at a pressure of about 140 atm. The membrane and electrode assembly (MEA) is then placed in the appropriate position between the current collectors. The external surface area of the Nafion (i.e., without the electrode) serves as a gasket to prevent any leakage of the reactant gases from the anode side to the cathode side or vice-versa. The current collector contains the flow fields for the gases.

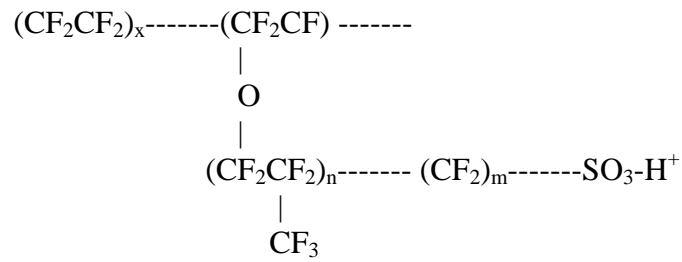
In respect to electrocatalysts, Pt or Pt alloys are the best ones to date. The reason is that the electrolyte environment is quite acidic (as strong as 2N sulfuric acid). Hence, it is not possible to use transition metals or their alloys. Other electrocatalysts have been investigated, but to date, these have not yielded the desired performance characteristics in respect to power density or lifetime.

The discovery of the perfluorosulfonic acid membrane by Dupont, Inc. made it possible to enhance the power density of a PEMFC by five to ten times. It is interesting to analyze the quantum jumps made in the development of proton conducting membranes from 1959 to 1980 (see Table 3.2). There are two reasons for the dominance of PEMFC technology with Nafion as compared with phenol sulfonic and polystyrene sulfonic acid membranes used previously. PFSAs, like Nafion, have a Teflon-like backbone except for side chains with ether like linkages, followed by FP2 groups prior to the sulfonic acid group (Figure 3.2). The high electronegativity of the

fluorine atom bonded to the sulfonic acid enhances the acidity of Nafion to that of a superacid like trifluoromethane sulfonic acid ($\text{CF}_3\text{SO}_3\text{H}$). C-F bonds are also highly electrochemically stable compared to C-H bonds (present in PSSAs and other C-H based polymeric acids), particularly at potentials in the range of operation of the oxygen electrode, enhancing the lifetime by about four orders of magnitude (see Table 3.2). High proton conductivity and high mechanical/chemical stabilities are prerequisites for proton conducting membranes for PEMFCs. Efforts were made successfully by Dow Chemical Company and Asahi Chemical Company to enhance proton conductivities in PFSA by some modification in the structures, i.e., altering the m and n parameters in the structure of the PFSA (Figure 3.2). The Nafion was impregnated into a supporting Teflon mesh, another major advance in PEMFC technology.

Table 3.2 The development of proton conductive membranes

Time	Membrane	Power density (kW/m ²)	Lifetime (thousands of Hours)
1959-1961	Phenol sulfonix	0.05-0.1	0.3-1
1962-1965	Polystyrene sulfonix	0.4-0.6	0.3-2
1966-1967	Polytrifluorostyrene sulfonix	0.75-0.8	1-10
1968-1970	Nafion (experimental)	0.8-1	1-100
1971-1980	Nafion (production)	6-8	10-100



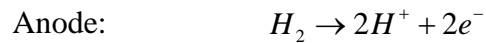
	N	m
ACIPLEX-S	0-2	2-5
DOW	0	2
NAFION	1	2
	EW	thickness
ACIPLEX-S1004	1000	120 μm
DOW	800	125 μm
NAFION	1100	100 μm

Figure 3.2 Basic structure and composition of some perfluorosulfonic acid membrane of DuPont, Dow, and Asahi Chemical.

3.2.3 Operation principle of PEM

A PEM fuel cell uses a simple chemical reaction to combine hydrogen and oxygen into water, producing electric current in the process. Figure 3.3 shows the flow diagram of PEM. More details of the mechanism occurred in PEM are summarized as follows:

- At the anode, hydrogen molecules give up electrons, forming hydrogen ions. This process is made possible by the platinum catalyst.



- The proton exchange membrane allows protons to flow through, but not electrons. As a result, the hydrogen ions flow directly through the proton exchange membrane to the cathode, while the electrons flow through an external circuit.
- As they travel to the cathode through the external circuit, the electrons produce electrical current. This current can perform useful work by powering any electrical device (such as an electric motor or a light bulb).

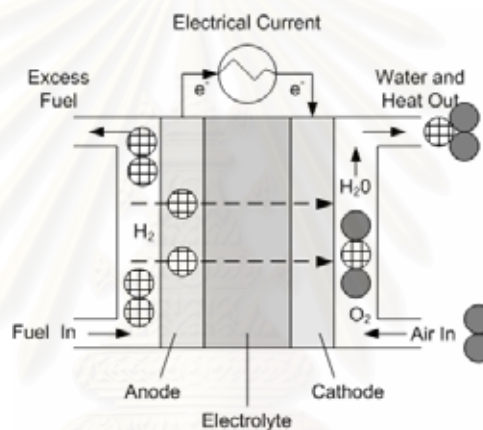
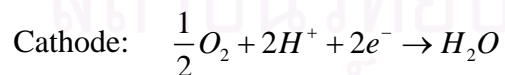
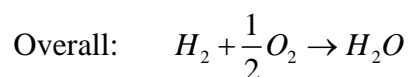


Figure 3.3 Flow diagram of polymer electrolyte fuel cell

- At the cathode, the electrons and hydrogen ions combine with oxygen to form water.



- In a fuel cell, hydrogen's natural tendency to oxidize and form water produces electricity and useful work.
- No pollution is produced and the only byproducts are water and heat.



CHAPTER IV

MATHEMATICAL MODEL OF PEMFC

A mathematical model is essential tool in the design of a PEMFC system. A mathematical model of PEMFC under isothermal condition is developed based on appropriate mass conservation and electrochemical. The model is used to predict cell behavior, i.e., gas composition, cell potential and current density, along the length of fuel cell for various cell configurations and operation conditions.

4.1 Mass balances

Physical phenomena occurring within a PEM fuel cell can in general be represented by the solution of conservation equations for mass, species and current transport. The complete mass conservation equations of PEM fuel cell are presented in this section. Mass balance of fuel cell requires that the sum of all mass input must be equal to the sum of all mass outputs. The inputs are the flows of fuel and oxidant plus water vapor present in those gases. The outputs are the flows of unused fuel and oxidant, plus water vapor present in those gases, plus any liquid water present in either fuel or oxidant exhaust. Figure 4.1 shows the schematic diagram of PEM fuel cell

The conservations of mass is established as follows:

Fuel channel:

$$\frac{\partial C_{\text{H}_2,f}}{\partial x} = \frac{1}{u_f} R_x \frac{1}{h_f} \quad (4.1)$$

$$\frac{\partial C_{\text{H}_2\text{O},f}}{\partial x} = \left(\frac{1}{u_f h_f} \right) N_w \quad (4.2)$$

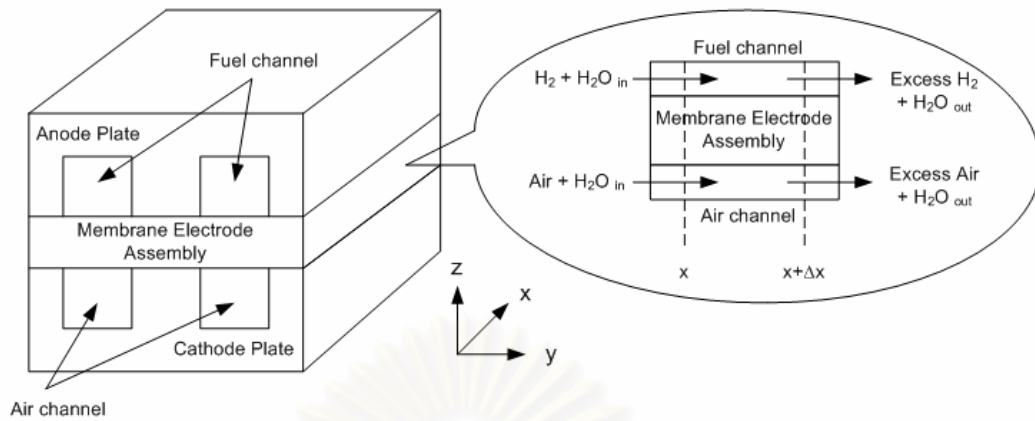


Figure 4.1 Schematic diagram of PEM fuel cell

Air channel:

$$\frac{\partial C_{O_2,a}}{\partial x} = \frac{1}{u_a} R_x \frac{1}{h_a} \quad (4.3)$$

It is noted that R_x is the rate of electrochemical reaction that can be expressed as:

$$R_x = -R_{H_2,a} = R_{H_2O,c} = -\frac{1}{2} R_{O_2,c} = \frac{i}{nF} \quad (4.4)$$

and N_w is the water vapor flux transport across the membrane electrode assembly (MEA) that can be explained by the combined effects of electro-osmosis drag force (n_D) and back diffusion (D_w) as shown in the following equation:

$$N_w = n_D \frac{i}{F} - D_w \frac{(C_{H_2O,a} - C_{H_2O,f})}{\delta} \quad (4.5)$$

In this study, transport properties of the electrolyte for Nafion membranes are considered. The electro-osmotic drag coefficient for water (n_d) in the membrane and the water diffusivity through the membrane are correlated with the water content of the membrane (λ) which is a function of the water activity (a) as:

$$a = \frac{X_w P}{P^{sat}} \quad (4.6)$$

$$\lambda = \begin{cases} 0.043 + 17.81a - 39.85a^2 + 36.0a^3 & \text{for } 0 < a \leq 1 \\ 14 + 1.4(a - 1) & \text{for } 1 < a \leq 3 \end{cases} \quad (4.7)$$

$$n_d = \begin{cases} 0.0049 + 2.02a_{anode} - 4.53a_{anode}^2 + 4.09a_{anode}^3 & \text{for } a_{anode} \leq 1 \\ 1.59 + 0.159(a_{anode} - 1) & \text{for } a_{anode} > 1 \end{cases} \quad (4.8)$$

$$D_{w,mem} = n_d 5.5 \times 10^{-11} \exp \left[2416 \left(\frac{1}{303} - \frac{1}{T} \right) \right] \quad (4.9)$$

For the two-phase model, water produced is assumed to be in the liquid phase. Considering a water vapor at the cathode channel, an additional term accounting for evaporation /condensation appears in the mass balance equation of the water vapor as follows:

$$R_w = k_c \frac{\varepsilon(1-s)}{RT} X_w (p_w - P^{sat}) q + k_v \frac{\varepsilon s \rho_w}{M_w} (p_w - P^{sat}) (1-q) \quad (4.10)$$

where R_w is the interfacial transfer of water between liquid water and vapor water. If the vapor pressure of water at the cathode side is more than the saturated vapor pressure, the water vapor will condense ($q = 1$). On the other hand, if the saturated vapor pressure is more than the partial pressure of vapor water, the liquid water will evaporate ($q = 0$).

Mass balances of water at the air channel are as follows:

Vapor water:

$$\frac{\partial C_{H_2O,a(v)}}{\partial x} = \left(\frac{1}{u_a h_a} \right) (N_w - R_w) \quad (4.11)$$

Liquid water:

$$\frac{\partial C_{H_2O,a(liq)}}{\partial x} = \left(\frac{1}{u_a h_a} \right) (R_x + R_w) \quad (4.12)$$

4.2 Theoretical fuel cell potential

In general, electrical work is a product of charge and potential:

$$W_{el} = qE \quad (4.13)$$

The total charge transferred in fuel cell reaction per mol of H₂ consumed is equal to:

$$q = nF \quad (4.14)$$

Electrical work is therefore:

$$W_{el} = nFE \quad (4.15)$$

The maximum amount of electrical energy generated in a fuel cell corresponds to Gibbs free energy, ΔG :

$$W_{el} = -\Delta G \quad (4.16)$$

The theoretical potential of fuel cell is then:

$$E = \frac{-\Delta G}{nF} \quad (4.17)$$

The theoretical cell potential (E_{thermo}) changes with an operating temperature as:

$$E = E_{thermo} = -\left(\frac{\Delta H}{nF} - \frac{T\Delta S}{nF}\right) \quad (4.18)$$

In general, fuel cell may operate at any pressure. For isothermal process, the change in Gibbs free energy due to the variation of the pressure may be shown as:

$$G = G_0 + RT \ln\left(\frac{P}{P_0}\right) \quad (4.19)$$

For the hydrogen/oxygen fuel cell reaction, the change in Gibbs free energy is the change between products and reactants:

$$\Delta G = \Delta G_0 + RT \ln \left(\frac{P_{H_2} P_{O_2}^{0.5}}{P_{H_2O}} \right) \quad (4.20)$$

This is known as the Nernst equation,

From the definition of the theoretical potential of fuel cell (Eq. (4.17)), Eq. (4.20) becomes:

$$E = E_{thermo} = E_0 + \frac{RT}{nF} \ln \left(\frac{P_{H_2} P_{O_2}^{0.5}}{P_{H_2O}} \right) \quad (4.21)$$

It is noted that when liquid water is produced in fuel cell, $P_{H_2O}=1$. From Eq. (4.21), it can be seen that at higher reactant pressure the cell potential is higher.

4.3 Voltage losses

If a fuel cell is supplied with reactant gases, but the electrical circuit is not closed, it will not generate any current, and one would expect the cell potential to be at, or at least close to, the theoretical cell potential for given conditions (temperature, pressure, and concentration of reactants). However, in practice this potential, which called the open circuit potential, is significantly lower than the theoretical potential, usually less than 1V. This suggests that there are some losses in the fuel cell even when no external current is generated. When the electrical circuit is closed with a load (such as a resistor) in it, the potential is expected to drop even further as a function of current being generated, due to unavoidable losses. There are different kinds of voltage losses in fuel cell caused by the following factors:

4.3.1 Activation polarization

Some voltage difference from equilibrium is needed to get the electrochemical reaction going. This is called activation polarization, and it is associated with sluggish electrode kinetics. These losses happen at both the anode and cathode; however, oxygen reduction requires much higher overpotentials, that is, it is a much slower reaction than hydrogen oxidation.

At relatively high negative overpotentials (i.e., potentials lower than the equilibrium potential), such as those at the fuel cell cathode, the first term in the Butler-Volmer equation becomes predominant, which allows for expression of potential as a function of current density (from Eq. (4.22)):

$$\Delta V_{act,c} = E_{r,c} - E_c = \frac{RT}{\alpha_c F} \ln \left(\frac{i}{i_{0,c}} \right) \quad (4.22)$$

Similarly, at the anode at positive overpotentials (i.e., higher than the equilibrium potential) the second term in the Butler-Volmer equation becomes predominant:

$$\Delta V_{act,a} = E_{r,a} - E_a = \frac{RT}{\alpha_a F} \ln \left(\frac{i}{i_{0,a}} \right) \quad (4.23)$$

In electrochemistry, the reversible potential of the hydrogen oxidation reaction is zero at all temperatures. That is why the standard hydrogen electrode is used as a reference electrode. Therefore, for hydrogen anodes $E_{r,a} = 0$ V. Activation polarization of the hydrogen oxidation reaction is much smaller than activation polarization of the oxygen reduction reaction.

A simplified way to show the activation losses is to use the so-called Tafel equation:

$$\Delta V_{act} = a + b \log(i) \quad (4.24)$$

- where $a = -2.3 \frac{RT}{\alpha F} \log(i)$, and $b = 2.3 \frac{RT}{\alpha F}$

If these activation polarizations were the only losses in a fuel cell, the cell potential would be:

$$E_{cell} = E_c - E_a = E_r - \Delta V_{act,c} - \Delta V_{act,a} \quad (4.25)$$

$$E_{cell} = E_r - \frac{RT}{\alpha_c F} \ln \left(\frac{i}{i_{0,c}} \right) - \frac{RT}{\alpha_a F} \ln \left(\frac{i}{i_{0,a}} \right) \quad (4.26)$$

If anode polarization is neglected, the previous equation becomes:

$$E_{cell} = E_r - \frac{RT}{\alpha F} \ln\left(\frac{i}{i_0}\right) \quad (4.27)$$

This has the same form as the Tafel Eq. (4.27).

4.3.2 Ohmic Losses

Ohmic losses occur because of resistance to the flow of ions in the electrolyte and resistance to the flow of electrons through the electrically conductive fuel cell components. These losses can be expressed by Ohm's law:

$$\Delta V_{ohm} = iR_i \quad (4.28)$$

where R_i is the total internal resistances (i.e., ionic, electronic, and contact resistances)

Electronic resistance is almost negligible, even when graphite or graphite/polymer composites are used as current collectors. Ionic and contact resistances are approximately of the same order of magnitude. Typical values for R_i are between 0.1 and 0.2 $\Omega \text{ cm}^2$.

As mentioned earlier, transport properties of the electrolyte for Nafion membranes are considered. The proton conductivity (K_{mem}) in the membrane are correlated with the water content of the membrane (λ).

$$K_{mem} = (0.5139\lambda - 0.326) \exp\left[1268\left(\frac{1}{303} - \frac{1}{T}\right)\right] \times 100 \quad (4.29)$$

To determine the ohmic loss of the membrane, membrane resistance could be calculated by the membrane conductivity and the membrane thickness as:

$$R_{mem} = \delta / K_{mem} \quad (4.30)$$

Following the Ohm's law, the ohmic loss of the membrane can be expressed by:

$$\eta_{ohmic} = iR_i \quad (4.31)$$

$$R_i = \delta\rho + \delta/K_{mem} \quad (4.32)$$

where ρ is the specific electronic resistance of membrane.

4.3.3 Concentration Polarization

Concentration polarization occurs when a reactant is rapidly consumed at the electrode by the electrochemical reaction so that concentration gradients are established. The electrochemical reaction potential changes with partial pressure of the reactants, and this relationship is given by the Nernst equation:

$$\Delta V = \frac{RT}{nF} \ln\left(\frac{C_B}{C_S}\right) \quad (4.33)$$

According to Fick's Law, the flux of reactant is proportional to concentration gradient:

$$N = \frac{D^{eff} (C_B - C_S)}{\delta} A \quad (4.34)$$

where D^{eff} is the effective diffusivity that relates between binary gas diffusion coefficient (D_{ij}) and the porosity of porous structure (ε) as:

$$D^{eff} = \varepsilon^{1.5} D_{ij} \quad (4.35)$$

where D_{ij} is a strong function of temperature, pressure, and the molecular weights of species i and j . At low pressures, nominal diffusivity can be estimated from the following equation based on the kinetic theory of gases.

$$D_{ij} = 3.640 \times 10^{-8} \left(\frac{T}{\sqrt{T_{c_i} T_{c_j}}} \right)^{2.334} \frac{(P_{c_i} P_{c_j})^{1/3}}{P} (T_{c_i} T_{c_j})^{5/12} \left(\frac{1}{M_i} + \frac{1}{M_j} \right)^{1/2} \quad (4.36)$$

The porosity (ε) of a gas diffusion can be calculated from real weight, thickness, and the density of solid phase (for carbon-based materials, ρ varies between 1.6 and 1.95 g/cm³).

$$\varepsilon = \frac{v_{mem}}{v_{total}} = \frac{1}{v_{total}} \frac{w_{mem}}{\rho_{mem}} \quad (4.37)$$

The weight fraction of platinum is:

$$f_{pt} = \frac{w_{pt}}{w_{pt} + w_c} \quad (4.38)$$

The weight fraction of membrane is:

$$f_{mem} = \frac{w_{mem}}{w_{pt} + w_c + w_{mem}} \quad (4.39)$$

Then,

$$\varepsilon = \frac{1}{v_{total} \rho_{mem}} \left\{ \frac{f_{mem}}{1 - f_{mem}} \right\} \frac{w_{pt}}{f_{pt}} \quad (4.40)$$

Rearranging Eq. (4.40), we obtain

$$\varepsilon = \frac{1}{\delta \rho_{mem}} \left\{ \frac{f_{mem}}{1 - f_{mem}} \right\} \frac{m_{pt}}{f_{pt}} \quad (4.41)$$

where ρ_{mem} is the membrane density that is related to water content in membrane as:

$$\rho_{mem} = 1000 \left(1.98 + \frac{0.0325\lambda}{(1+0.0648\lambda)} \right) \quad (4.42)$$

It is noted that if fuel cell has flooding or membrane has much water, it results in higher membrane density and the porosity will decrease. In addition, if water flooding in cell occurs, the membrane thickness will increase due to the addition of water film thickness. The water film thickness can be expressed as follows:

$$\delta_{w_mem} = \frac{r_{gg}}{3\rho_{mem}} \frac{(f_{mem}/(1-f_{mem}))(1/(1-\rho_{mem}))}{(f_{pt}/\rho_{pt}) + ((1-f_{pt})/\rho_{pt})(f_{mem}/(1-f_{mem})\rho_{mem})} \quad (4.43)$$

Thus, the total thickness when using the two-phase model is:

$$\delta = \delta_{soild} + \delta_{w_mem} \quad (4.44)$$

Under steady state condition, the rate at which the reactant species is consumed in the electro-chemical reaction is equal to the diffusion flux:

$$N = \frac{I}{nF} \quad (4.45)$$

By combining Eqs. (4.34) and (4.45), the following relationship is obtained:

$$i = \frac{nF \cdot D \cdot (C_B - C_S)}{\delta} \quad (4.46)$$

The reactant concentration at the catalyst surface thus depends on current density; the higher the current density, the lower the surface concentration. The surface concentration reaches zero when the rate of consumption exceeds the diffusion rate; the reactant is consumed faster than it can reach the surface. Current density at which this happens is called the limiting current density. A fuel cell cannot produce more than the limiting current because there are no reactants at the catalyst surface. Therefore, for $C_S = 0$, $i = i_L$, and the limiting current density is then:

$$i_L = \frac{nFDC_B}{\delta} \quad (4.47)$$

As a result, a relationship for the voltage loss due to concentration polarization is obtained:

$$\Delta V_{conc} = \frac{RT}{nF} \ln\left(\frac{i_L}{i_L - i}\right) \quad (4.48)$$

4.3.4 The Actual Voltage of Fuel Cell

The real voltage output of a fuel cell could be written by starting with the thermodynamically predicted voltage and then subtracting the various over-voltage losses as:

$$V = E_{thermo} - \eta_{act} - \eta_{ohmic} - \eta_{conc} \quad (4.49)$$

The net fuel cell current density – voltage (i-V) can be written as:

$$V = E_{thermo} - \frac{RT}{\alpha F} \ln\left(\frac{i}{i_0}\right) - iR_i - \frac{RT}{nF} \ln\left(\frac{i_L}{i_L - i}\right) \quad (4.50)$$

Figure 4.1 shows a typical electrical characteristic of fuel cell.

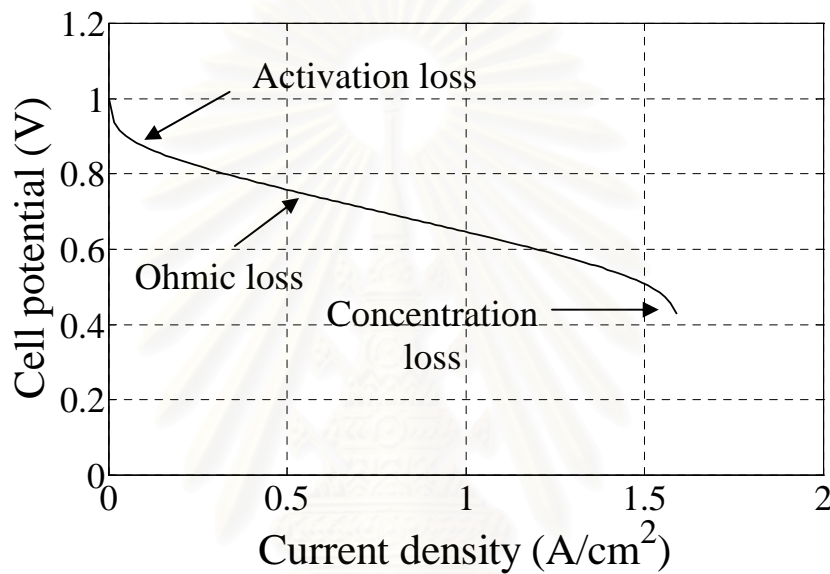


Figure 4.2 I-V curve of a polymer electrolyte membrane fuel cell

4.4 Power Generation

The power output (P_{out}) of fuel cell is the product of the voltage and current:

$$P_{out} = IV \quad (4.51)$$

For calculation, we need use current density to satisfy with another equation, so the Eq. (4.51) will become:

$$P_D = iV \quad (4.52)$$

The power density increase as the current density is increased until a maximum power density reached. Afterward, the power density is reduced because cell voltage is insufficient to maintain the power density.

4.5 Efficiency of Cell

The efficiency of any energy conversion device is defined as the ratio between useful energy output and energy input. In case of a fuel cell, the useful energy output is the electrical energy produced, and energy input is the enthalpy of hydrogen (hydrogen's higher heating value or hydrogen's lower heating value). The use of lower heating value is justified by water vapor being produced in the process, but is thermodynamically more correct to use the higher heating value, because it accounts for all the energy available and it is consistent with the definition of the efficiency. Assuming that all of the Gibbs free energy can be converted into electrical energy,

The efficiency of fuel cell is:

$$\eta_{eff} = \frac{\Delta G}{\Delta H} \quad (4.53)$$

The maximum possible (theoretical) efficiency of fuel cell is:

$$\eta_{eff} = \frac{\Delta G}{\Delta H} = \frac{237.34}{286.02} = 83\% \quad (4.54)$$

Then

$$\eta_{eff} = \frac{\frac{-\Delta G}{nF}}{\frac{-\Delta H}{nF}} = \frac{1.23}{1.482} = 83\% \quad (4.55)$$

Following this approach, the cell efficiency can be calculated as:

$$\eta_{eff} = \frac{V_{cell}}{1.482} \quad (4.56)$$

CHAPTER V

SIMULATION RESULTS AND DISCUSSION

In this chapter, the influences of operating parameters on PEMFC performance under isothermal and steady-state conditions are presented. Mathematical model of PEMFC described in Chapter IV is used to investigate the electrochemical characteristics of fuel cell.

5.1 Model validation

The PEM fuel cell consisting of the mass balances describing gas composition variation along the fuel and air channel and the electrochemical model as presented in Chapter IV is first validated with data obtained from literature (Liu et al., 2005). In their study, hydrogen gas with 90% relative humidity and air with 90% relative humidity are fed through a narrow fuel (at the anode side) and air (at the cathode side) channels, respectively. Nafion membrane is used in PEM fuel cell. The electrode porosity of 0.4, the operating temperature of 70 °C, and the operating pressure of 2 atm are taken to be the same as given by Liu et al. (2005). All the physical parameters used in the simulation are listed in Table 5.1.

Figure 5.1 shows the comparison of the model prediction using a single phase PEMFC model and experimental result. It can be seen that the proposed model can predict the cell characteristics very well.

Table 5.1 Model parameters used in the simulation

Parameters	Symbol	Value	Unit
Channel width	w	0.002	m
Channel length	L	0.25	m
Membrane thickness	δ	2.5×10^{-4}	m
Dry membrane density	$\rho_{dry,mem}$	2000	kg/ m ³
Membrane equivalent weight	M_{mem}	1.1	kg/mol
Specific resistance of membrane	ρ_{mem}	0.5	Ω m
Anode transfer coefficient	α_{an}	0.5	-
Cathode transfer coefficient	α_{ca}	2	-
Anode exchange current density	i_0^{an}	1.4×10^8	A/m ²
Cathode exchange current density	i_0^{ca}	5.0×10^{-4}	A/m ²
Condensation rate coefficient	k_c	100	s ⁻¹
Evaporation rate coefficient	k_v	100	s ⁻¹ atm ⁻¹
Liquid saturation	s	0.2	
Weight fraction of Pt on carbon	f_{pt}	0.2	
Weight fraction of ionomer	f_{mem}	0.25	
Pt loading inside the catalyst layer	m_{pt}	0.2	kg Pt/ m ²

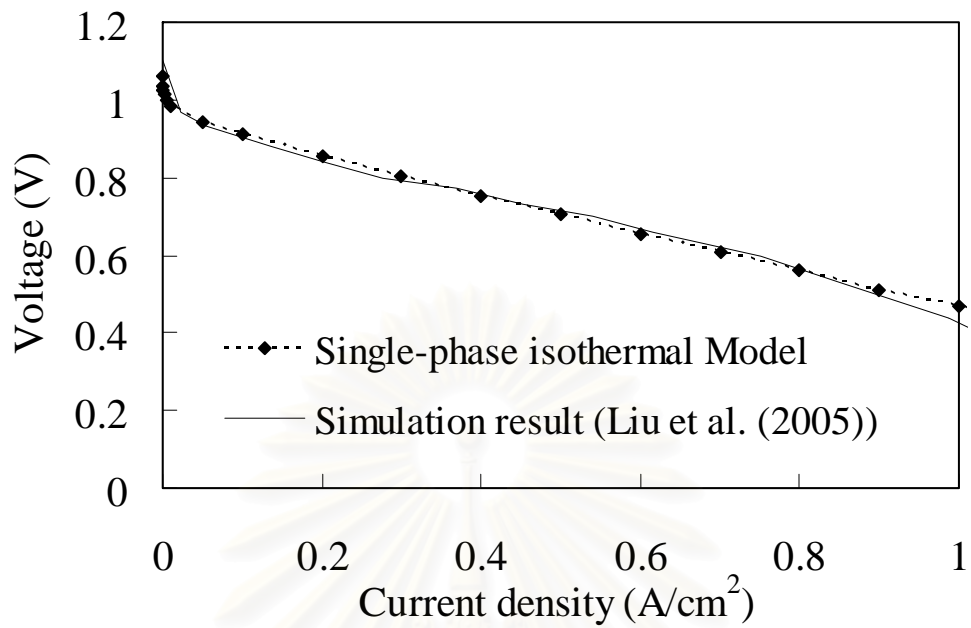


Figure 5.1 Comparison between model prediction and experimental data (Liu et al., 2005).

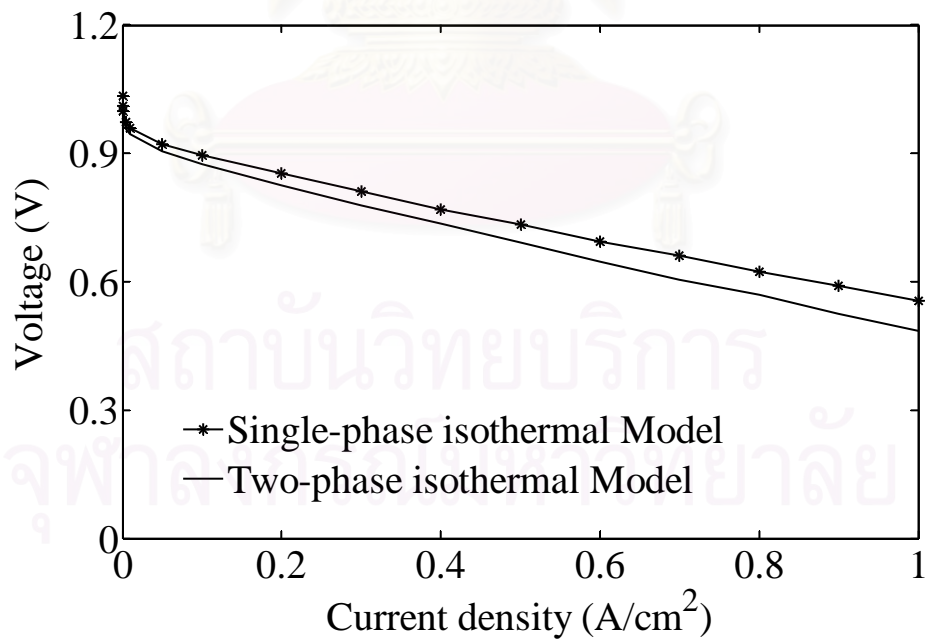


Figure 5.2 Comparison between a single-phase and two-phase PEMFC model.

Under the same operating condition of PEMFC as given in Liu et al., (2005), simulations of a PEMFC based on a single phase model and a two-phase model are compared in Figure 5.2. It is noted that the single phase model assumes that the water produced by an electrochemical reaction at the cathode is in a vapor form whereas it is in a liquid form in the two-phase model. From the polarization curve shown in Figure 5.2, it is found that the cell performance predicted by a two-phase model is lower than that obtained from the single phase model. Since the two-phase model accounts for the flooding effect on the gaseous reactant transport, an amount of oxygen permeated to the catalyst layer is lower. In addition, the liquid water causes higher ionic membrane resistances, thus leading to an increase in the ohmic loss. This result demonstrates the effect of the liquid water on the overall cell performance.

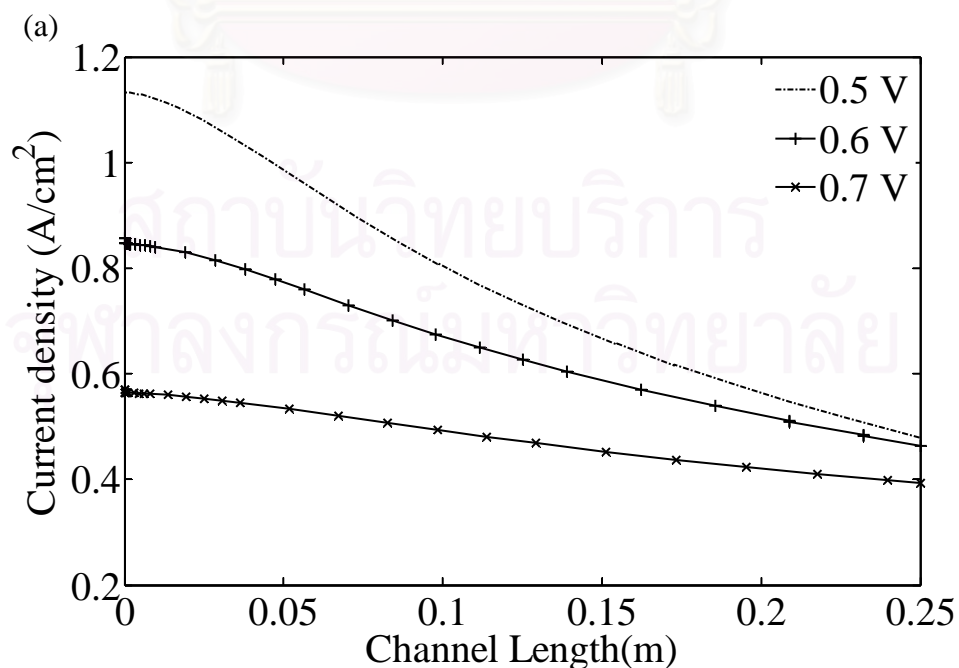
5.2 Performance of PEMFC at standard condition

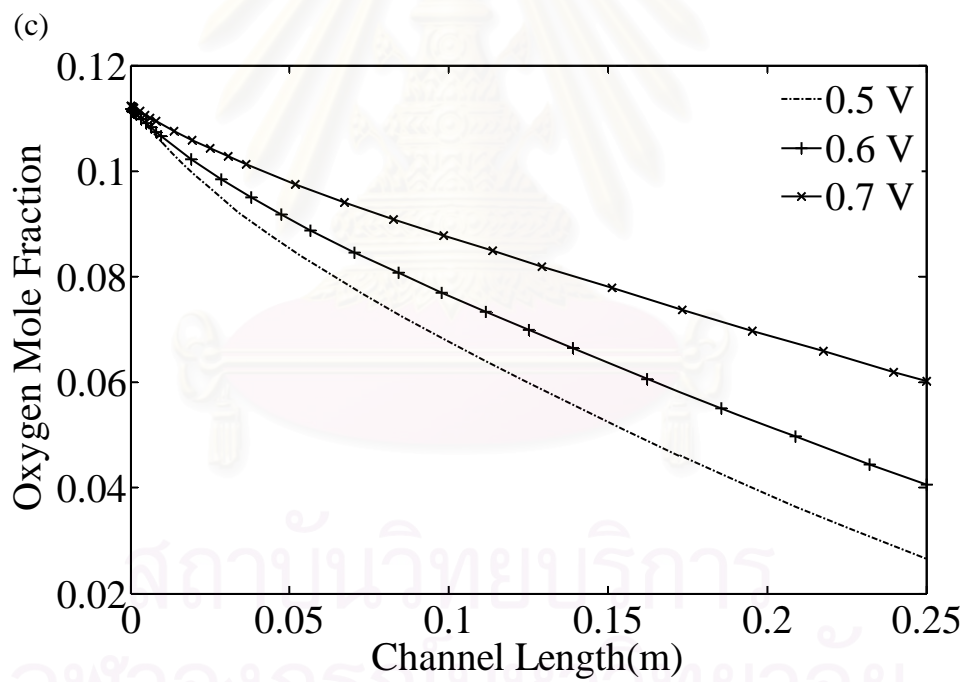
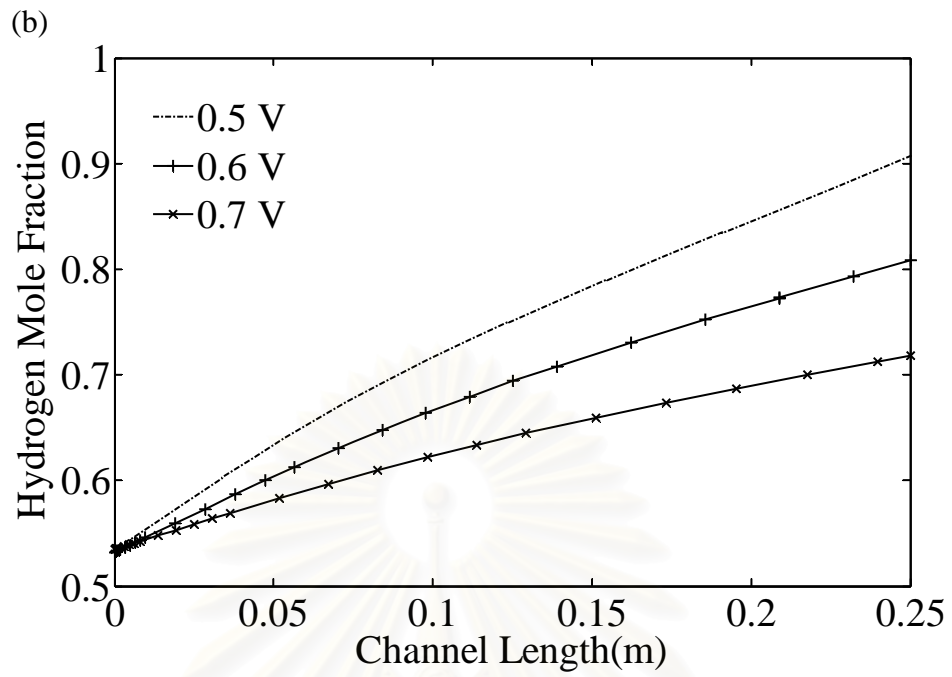
In the next section, the performance analysis of PEMFC using the two-phase model is performed under isothermal and steady state condition. Table 5.2 shows the operating conditions of PEMFC at the standard condition. Fully humidified hydrogen and air are fed to PEMFC at the fuel and air channels, respectively.

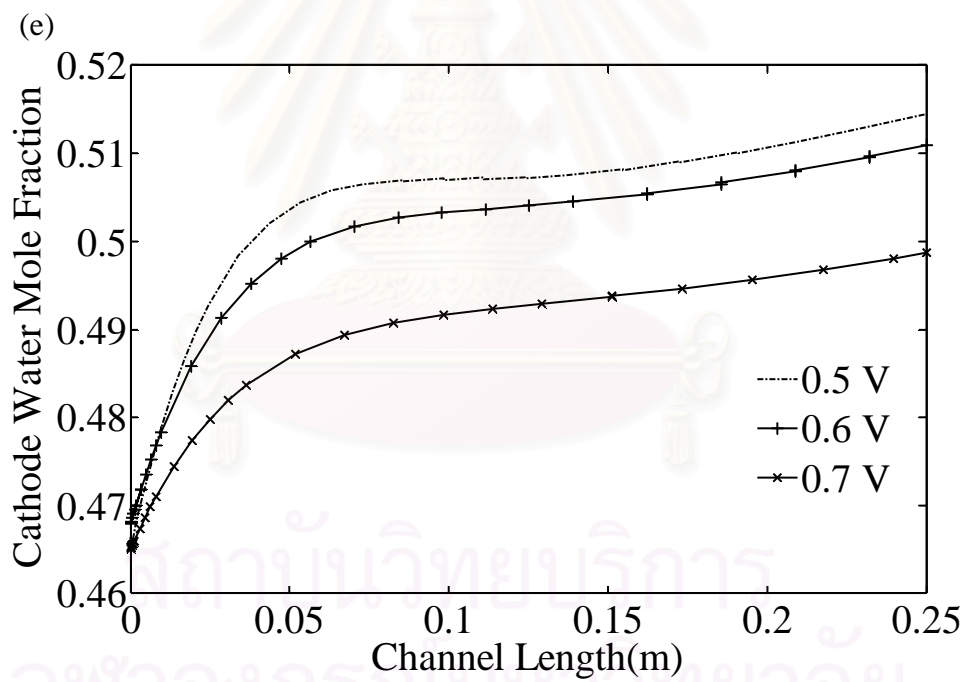
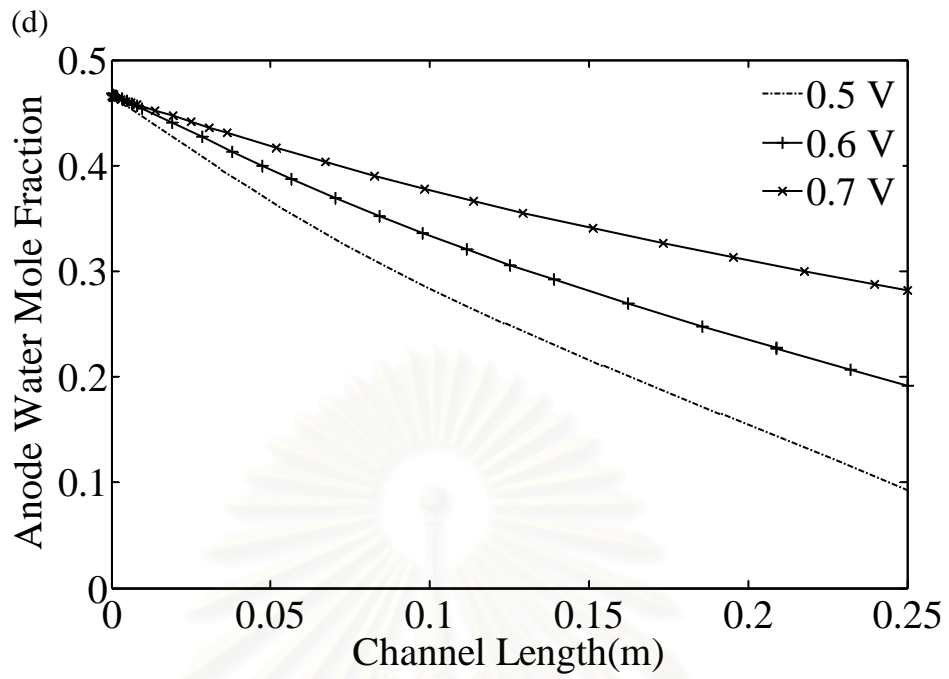
Table 5.2 Operation conditions of PEMFC at the standard condition

Parameters	Symbol	Value	Unit
Temperature of fuel cell	T	353.15	K
Inlet anode temperature	T _{an}	353.15	K
Inlet cathode temperature	T _{ca}	353.15	K
Relative humidity of reactants	RH	100	%
Cell pressure	P	1	atm
Volumetric flow rate of inlet anode gas	F _{an}	1.67 x 10 ⁻⁶	m ³ /s
Volumetric flow rate of inlet cathode gas	F _{ca}	3.33 x 10 ⁻⁶	m ³ /s
Electrode porosity	ε	0.4	-

Figure 5.3(a)-(f) show the distribution of current density, mole fraction of hydrogen, oxygen, water, and membrane conductivity along the flow direction at different operating cell voltage. It is found from Figure 5.3(a) that the current density decreases along the flow channel direction. This is due to the depletion of reactants (hydrogen and oxygen) as shown in Figures 5.3(b)-(c). It is noted that although hydrogen is consumed by the electrochemical reaction at the anode channel to generate the electricity, the mole fraction of hydrogen is increased as can be seen in Figure 5.3(b). This is because of a high decrease in vapor water in the anode channel due to the effect of the electro-osmosis drag force as shown in Figures 5.3(d). Figure 5.3(e) illustrates an increase in the mole fraction of vapor water at the channel inlet since vapor water is transferred from the anode to the cathode channel by the electro osmosis drag force and derived from the vaporization of liquid water generated by the electrochemical reaction. Since the water content in membrane decreases due to more vapor water transported across the membrane, the membrane ionic conductivity decreases as shown in Figure 5.3(f).







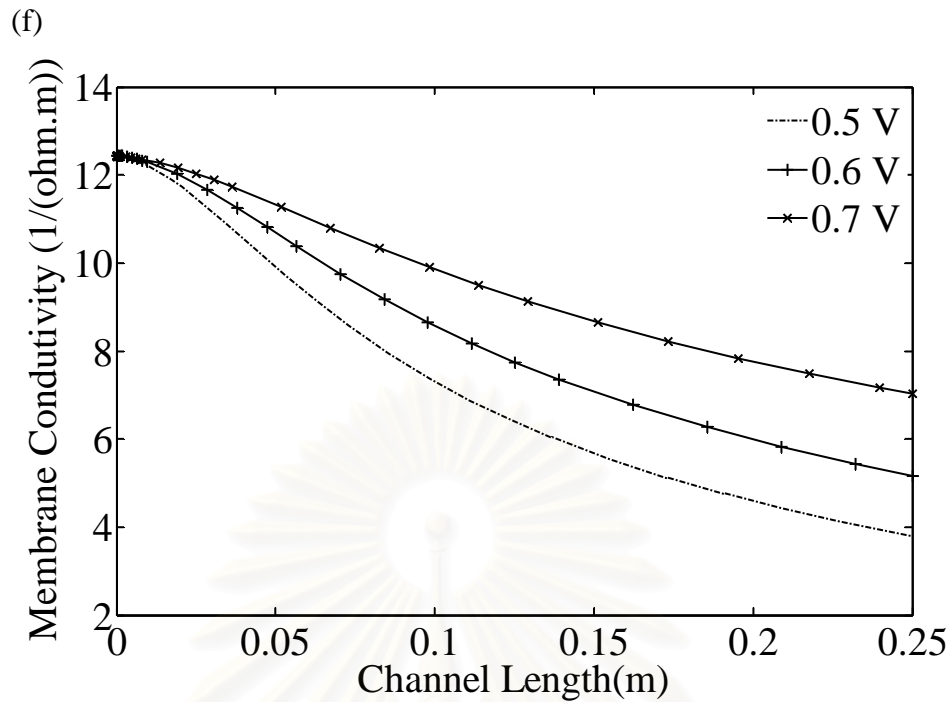
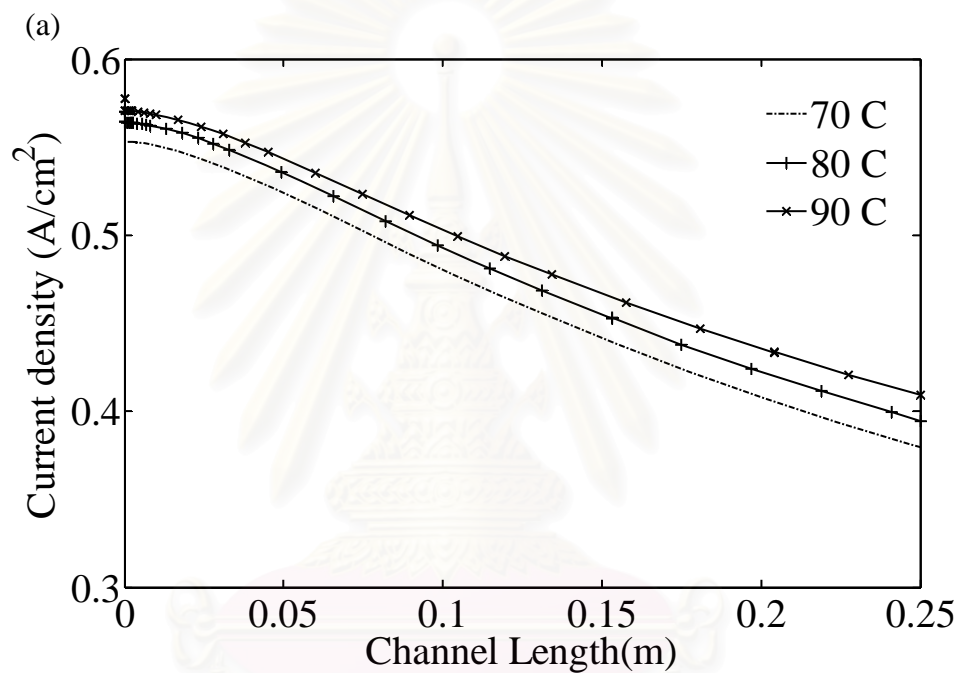


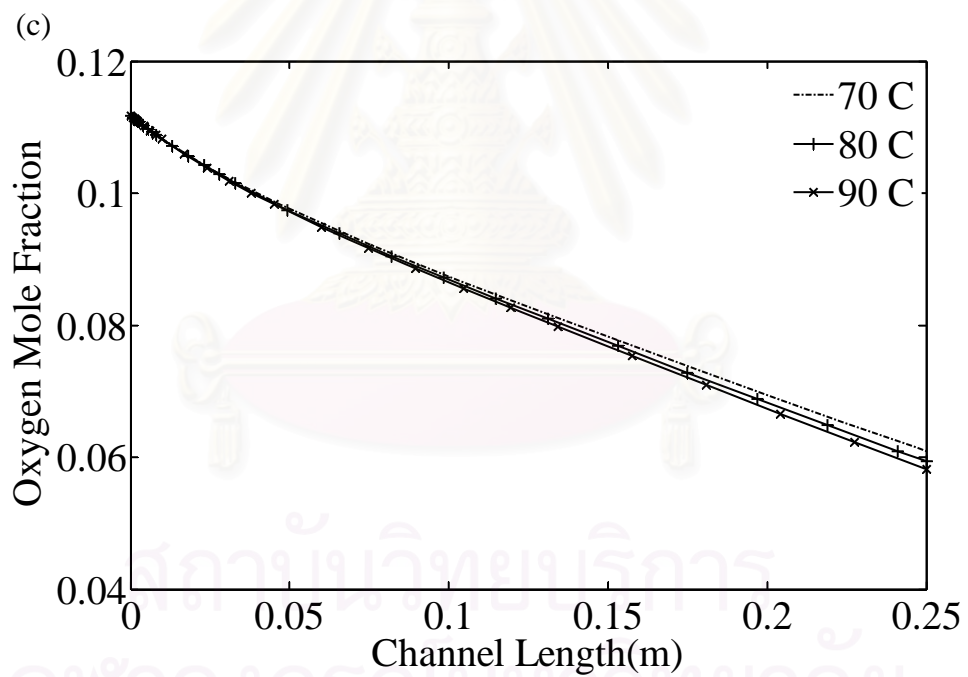
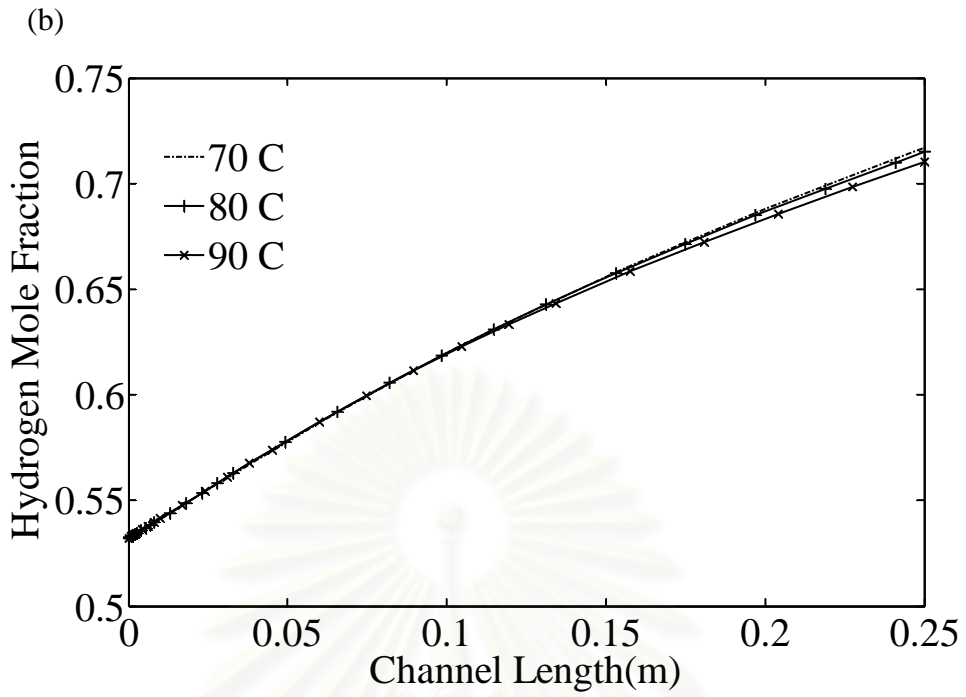
Figure 5.3 Profiles along the cell channel: (a) Current density, (b) hydrogen mole fraction at the anode, (c) oxygen mole fraction at the cathode, (d) water mole fraction at the anode, (e) water mole fraction at the cathode, and (f) Membrane Conductivity.

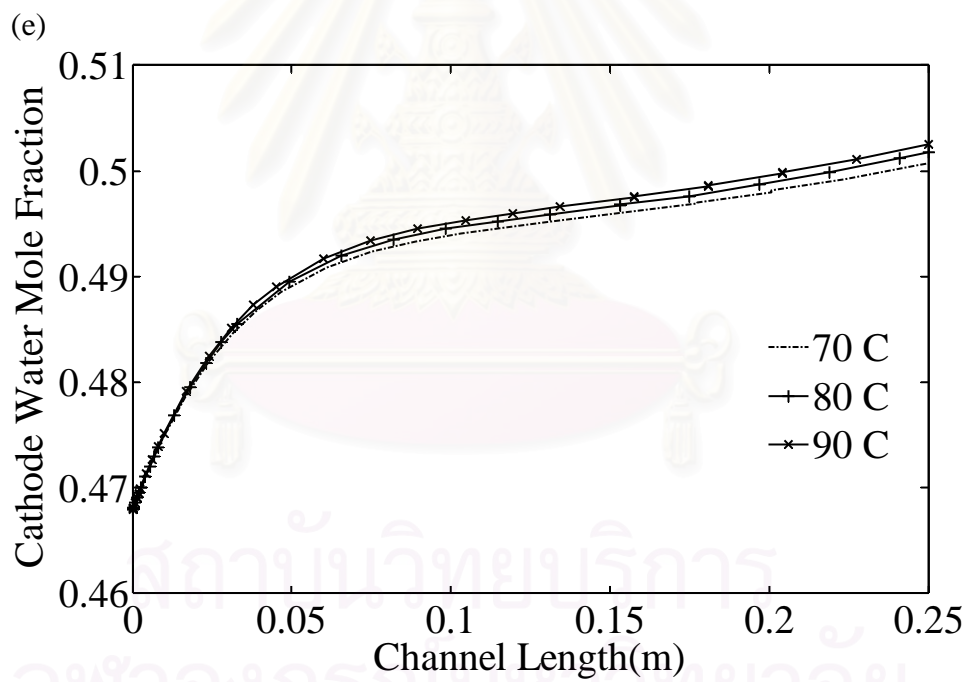
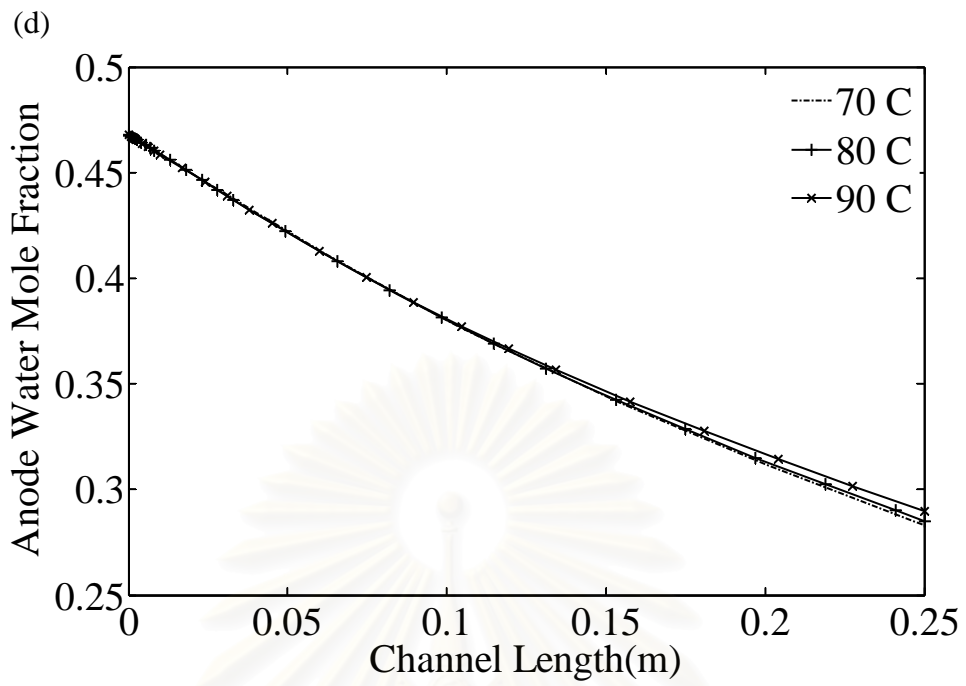
5.3 Effect of operating temperature

Figure 5.4(a)-(f) shows the distribution of current density, mole fraction of hydrogen, oxygen, water, and membrane conductivity along the flow direction at different operating temperature. It is found from Figure 5.4(a) that the current density decreases along the flow channel direction. This is due to the depletion of reactants (hydrogen and oxygen) as shown in Figures 5.4(b)-(c). At the same operating voltage of 0.7 V, more current density can be produced when the cell is operated at higher temperatures. However, an increase in operating temperatures has a slight effect on the variation of hydrogen, oxygen and water. It is noted that although hydrogen is consumed by the electrochemical reaction at the anode channel to generate the electricity, the mole fraction of hydrogen is increased as can be seen in Figure 5.4(b). This is because of a higher decrease in water vapor in the anode channel due to the effect of the electro-osmosis drag force as in Figures 5.4(d). As more water vapor

transports through the membrane to the cathode side by the electro osmosis drag force and some liquid water generated by electrochemical reactions at the cathode vaporizes, the fraction of water vapor at the cathode increases (Figure 5.4(e)). Due to a decrease in the water content of the membrane, the membrane ionic conductivity decreases as shown in Figure 5.3(f). Figure 5.3(f) show the operating temperature has a significant influence on the membrane ionic conductivity.







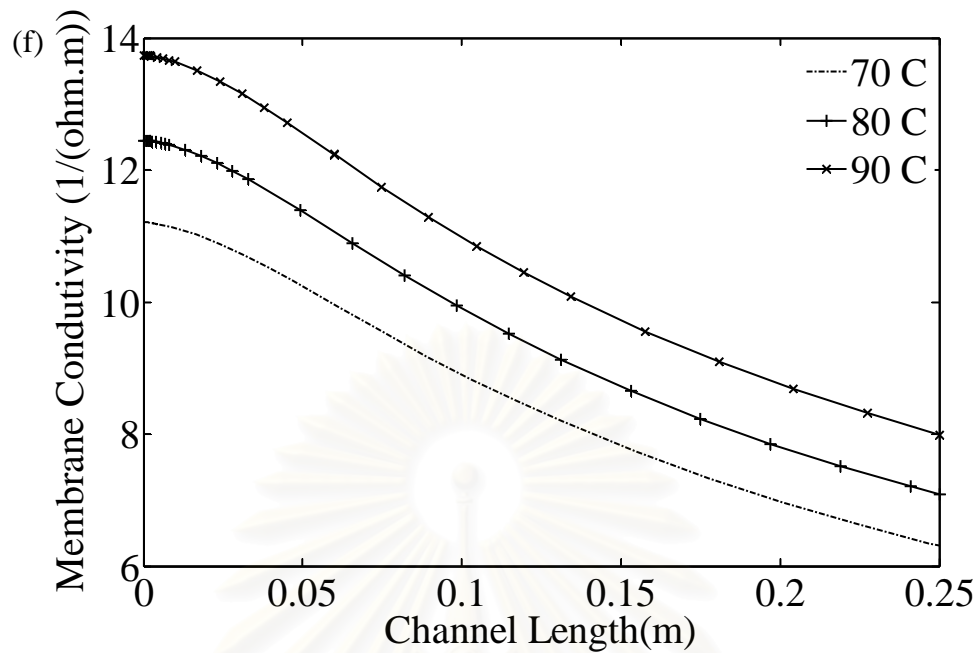


Figure 5.4 Profiles along the cell channel: (a) Current density, (b) Anode hydrogen mole fraction, (c) Cathode oxygen mole fraction, (d) Anode water mole fraction, (e) Cathode water mole fraction, and (f) Membrane Conductivity

The characteristic curve of cell voltage and power density for PEMFC at different operating temperature is presented in Figure 5.5(a)-(b). As expected, the cell performance increases with increasing operating temperature. This is due to the decreased mass transport resistance and ohmic loss.

สถาบันวิทยบริการ
จุฬาลงกรณ์มหาวิทยาลัย

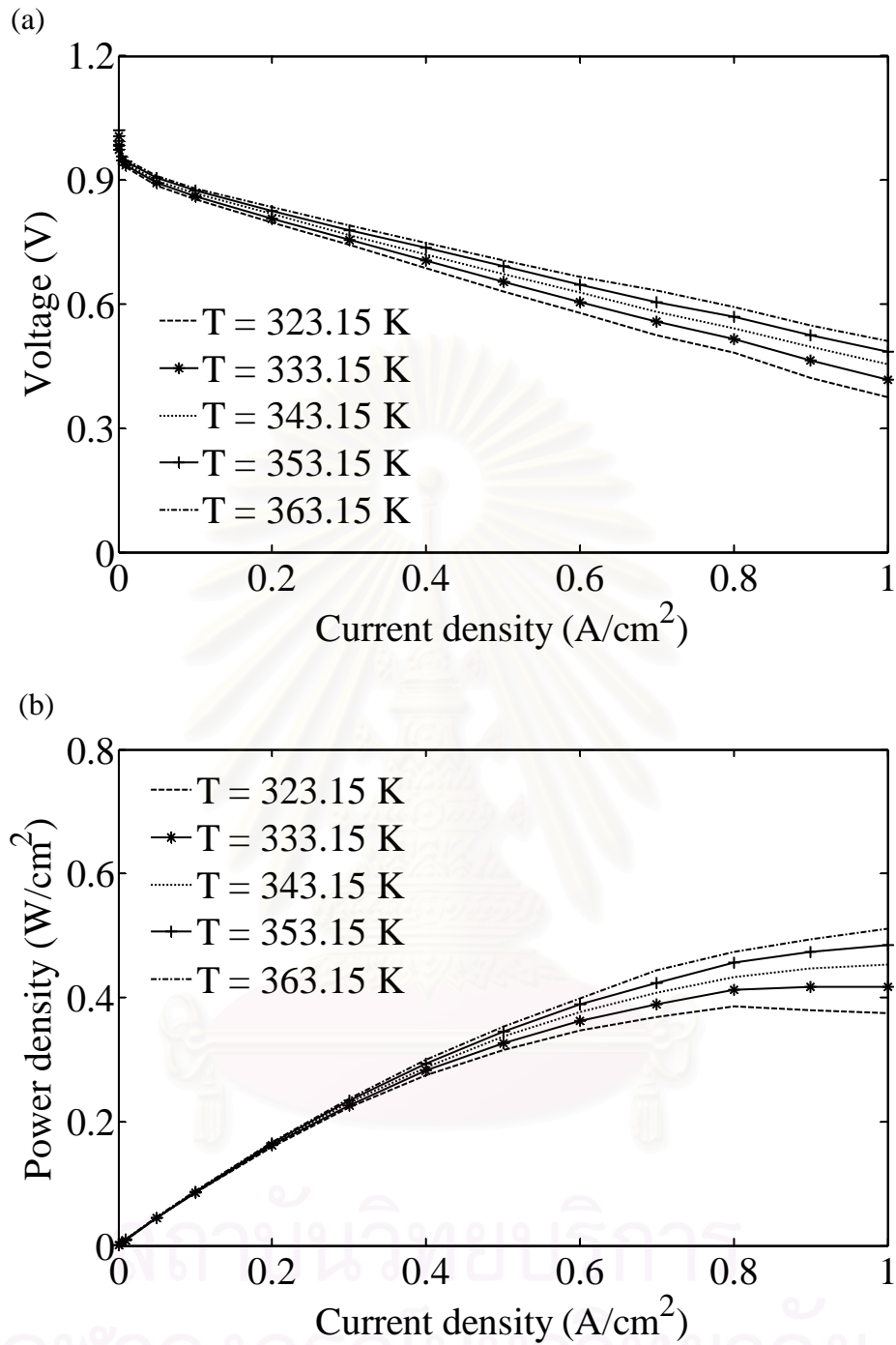


Figure 5.5 Effects of operating temperature at different current density on (a) cell voltage and (b) power density.

5.4 Effect of gas humidity

In this section, the effect of the relative humidity of inlet gas at the anode and cathode on cell performance is studied. Figures 5.6-5.13 show the distribution of current density, mole fraction of hydrogen, oxygen, water, membrane conductivity, membrane resistance loss, and cathode concentration loss along the flow direction of PEMFC at different relative humidity of inlet gas (50%, 75% and 100%) at the anode and cathode channels.

From Figure 5.6, it is found that when the humidified fuel gas with higher relative humidity is fed to PEMFC operated at the 0.7 V, the current density obtained increases as high vapor water in fuel gas cause the membrane to have more water content. This results in higher gas diffusivity and membrane conductivity. On the other hand, when hydrogen or air with higher relative humidity is used as fuel or oxidant, respectively, the current density is decreased due to the lower mole fraction of hydrogen at the anode or oxygen at the cathode as can be seen in Figures 5.7-5.8. Figure 5.9 illustrates the decrease of water vapor in the anode channel due to the effect of the electro-osmosis drag force. This leads to an increase in water vapor at the cathode. The results indicate that high humidified fuel and air cause an increase of vapor activity at both the electrodes and thus, increasing water content in membrane and the membrane ionic conductivity (Figure 5.11). The increased membrane ionic conductivity decreases the membrane resistance loss as can be seen in Figure 5.12. However, it is found from Figure 5.13 that the cathode concentration loss increases when fuel and air with high relative humidity are fed to PEMFC due to the decrease of oxygen diffusivity, leading to mass transport limitations.

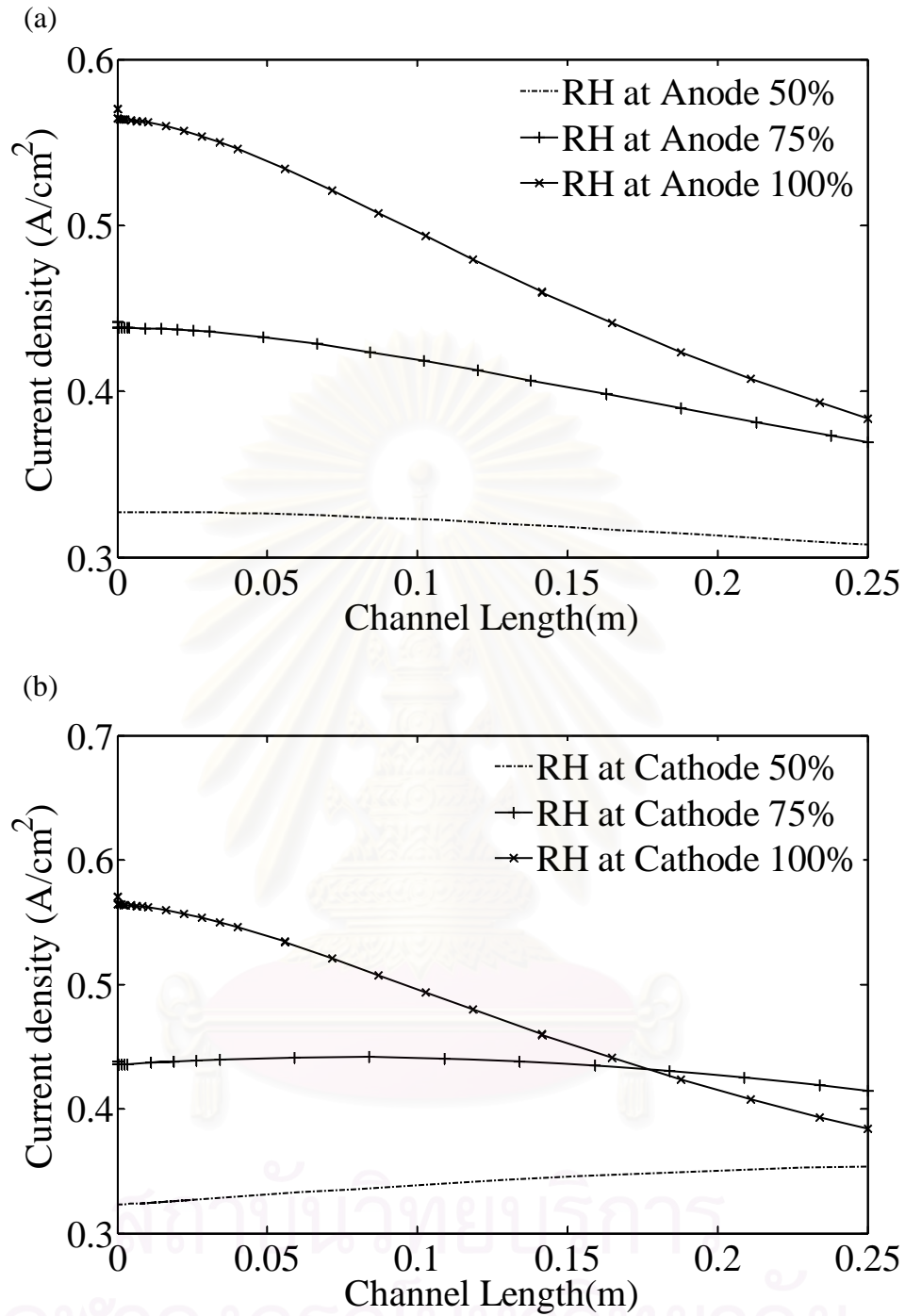


Figure 5.6 Distribution of current density along the cell channel at different gas inlet humidity at (a) anode channel and (b) cathode channel.

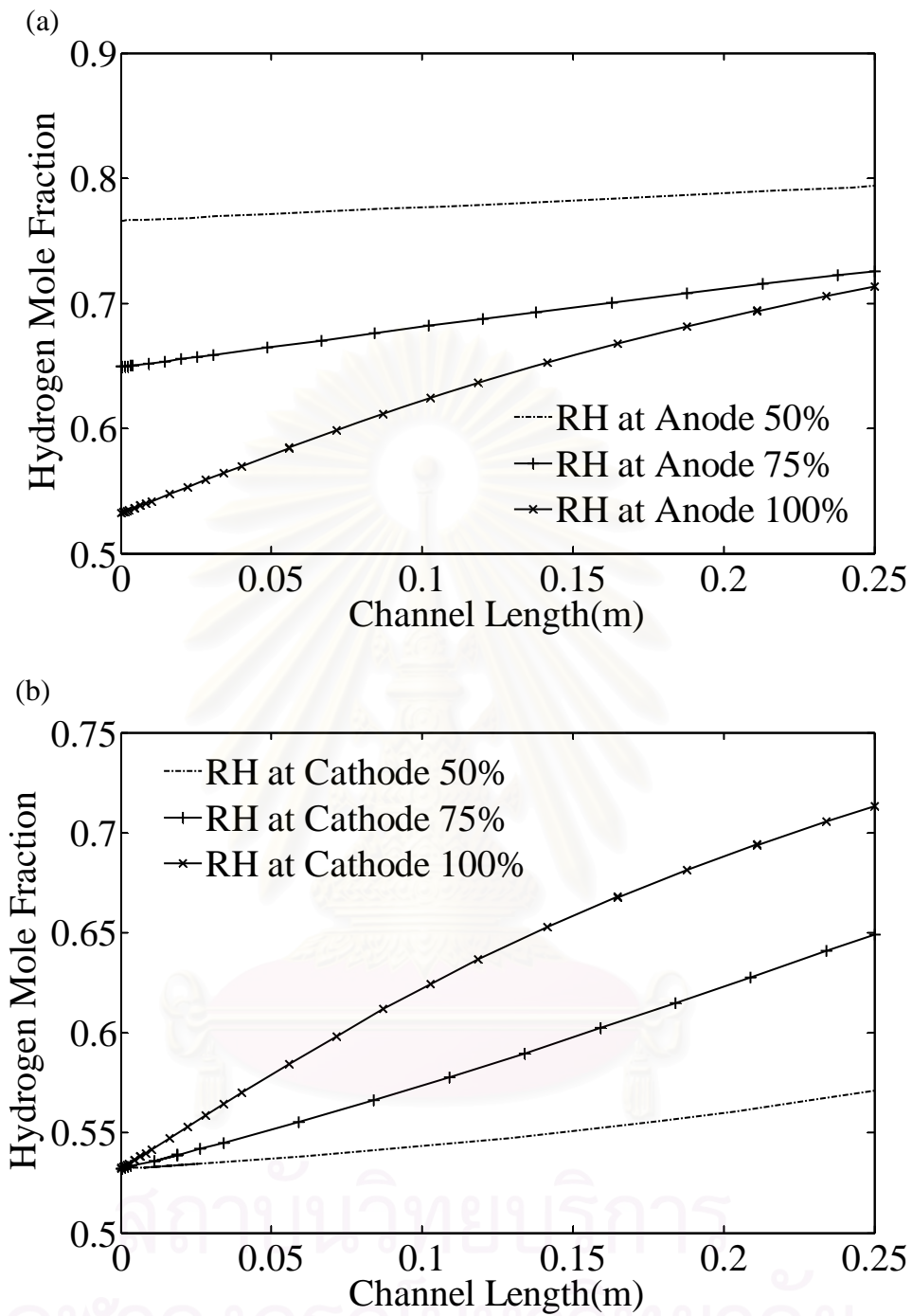


Figure 5.7 Distribution of hydrogen along the cell channel at different gas inlet humidity at (a) anode channel and (b) cathode channel.

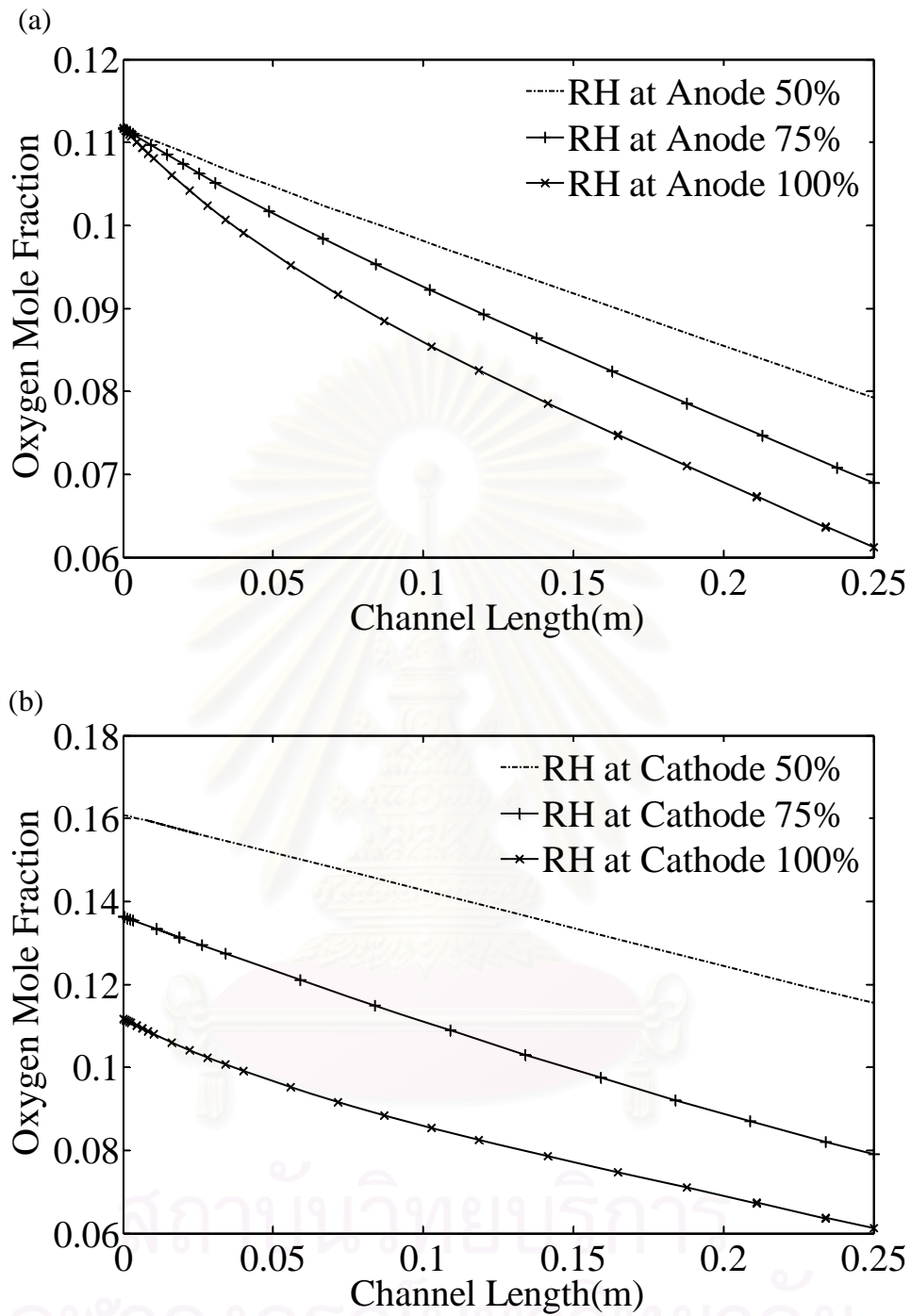


Figure 5.8 Distribution of oxygen along the cell channel at different gas inlet humidity at (a) anode channel and (b) cathode channel.

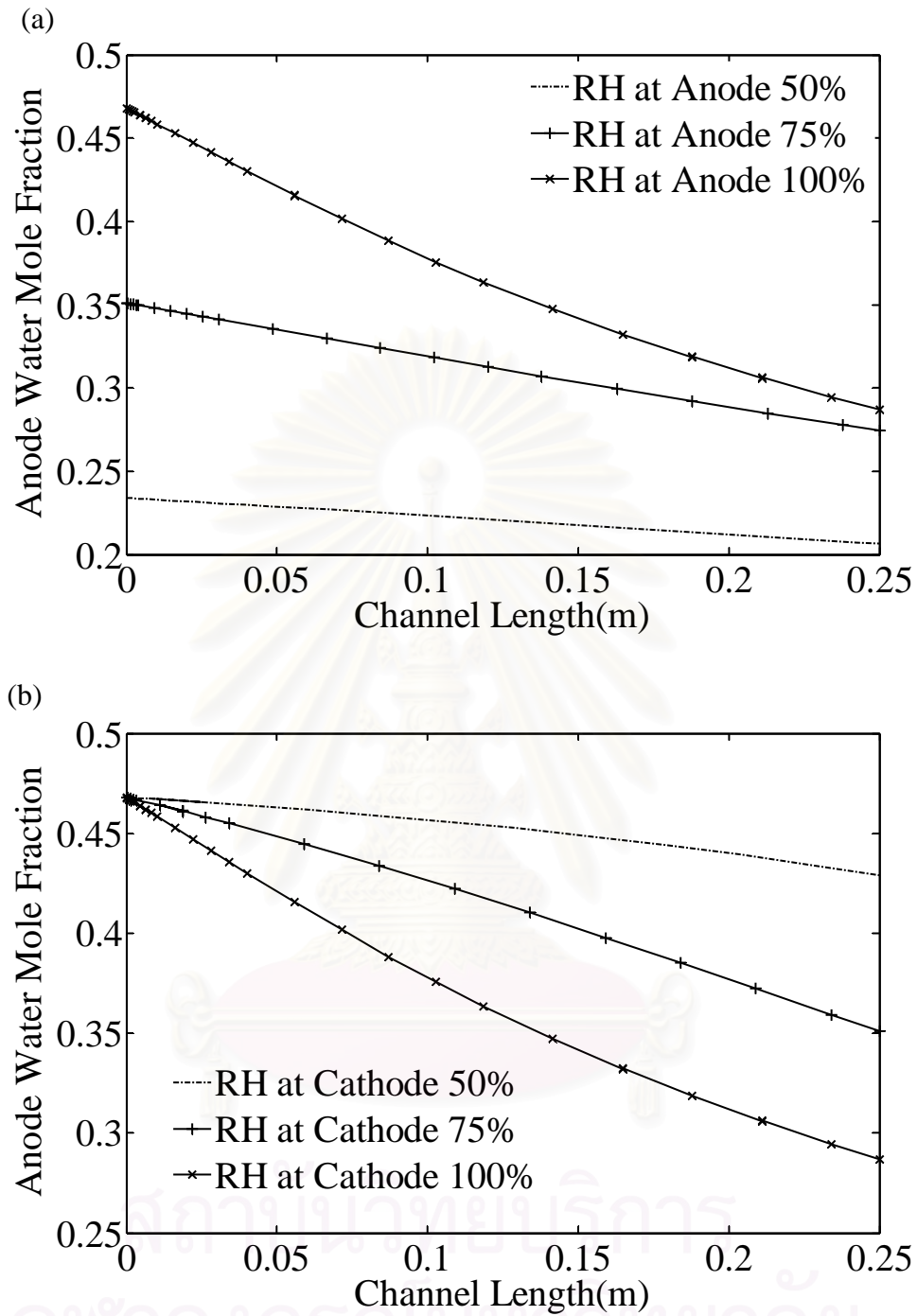


Figure 5.9 Distribution of anode vapor water along the cell channel at different gas inlet humidity at (a) anode channel and (b) cathode channel.

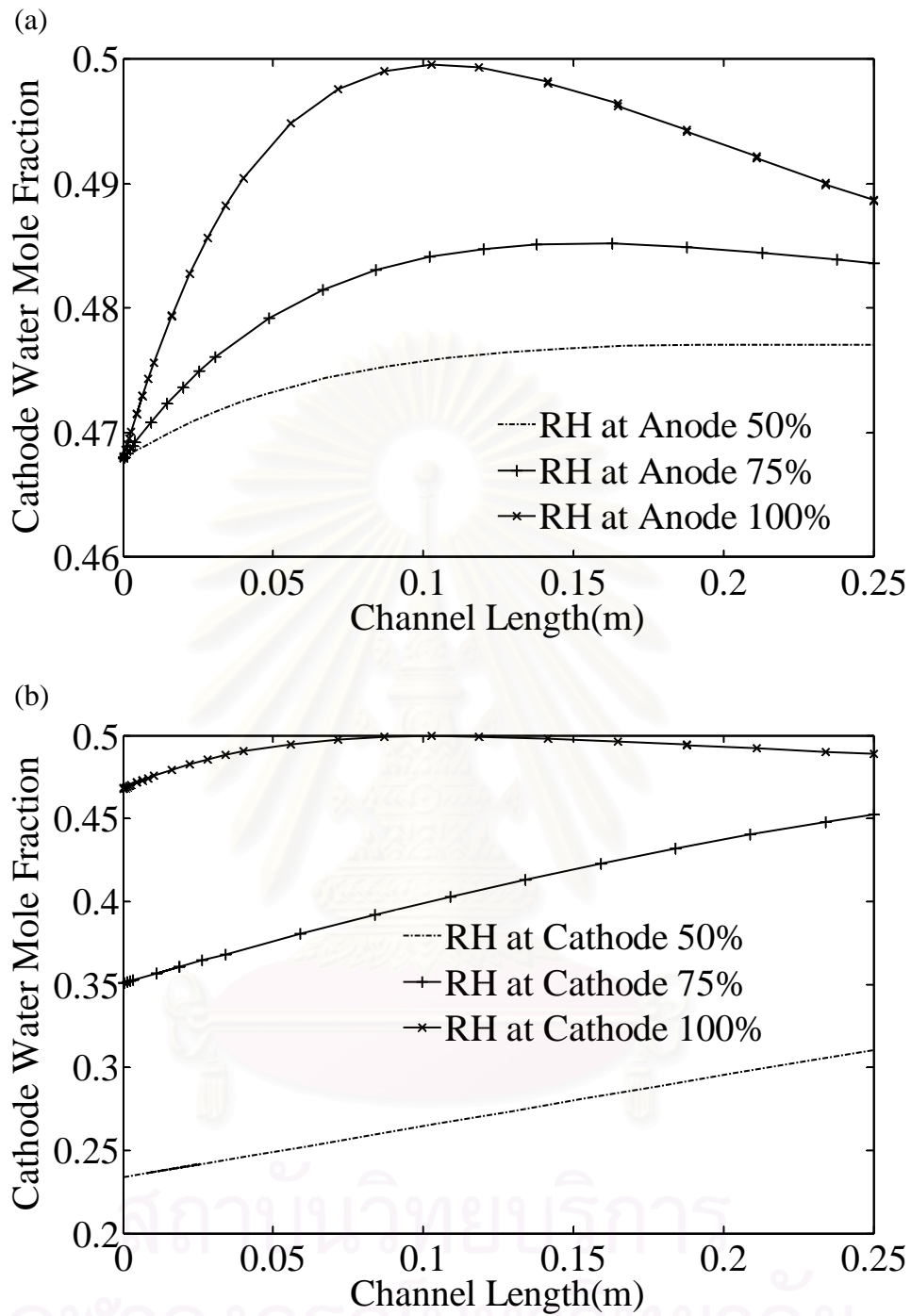


Figure 5.10 Distribution of cathode vapor water along the cell channel at different gas inlet humidity at (a) anode channel and (b) cathode channel.

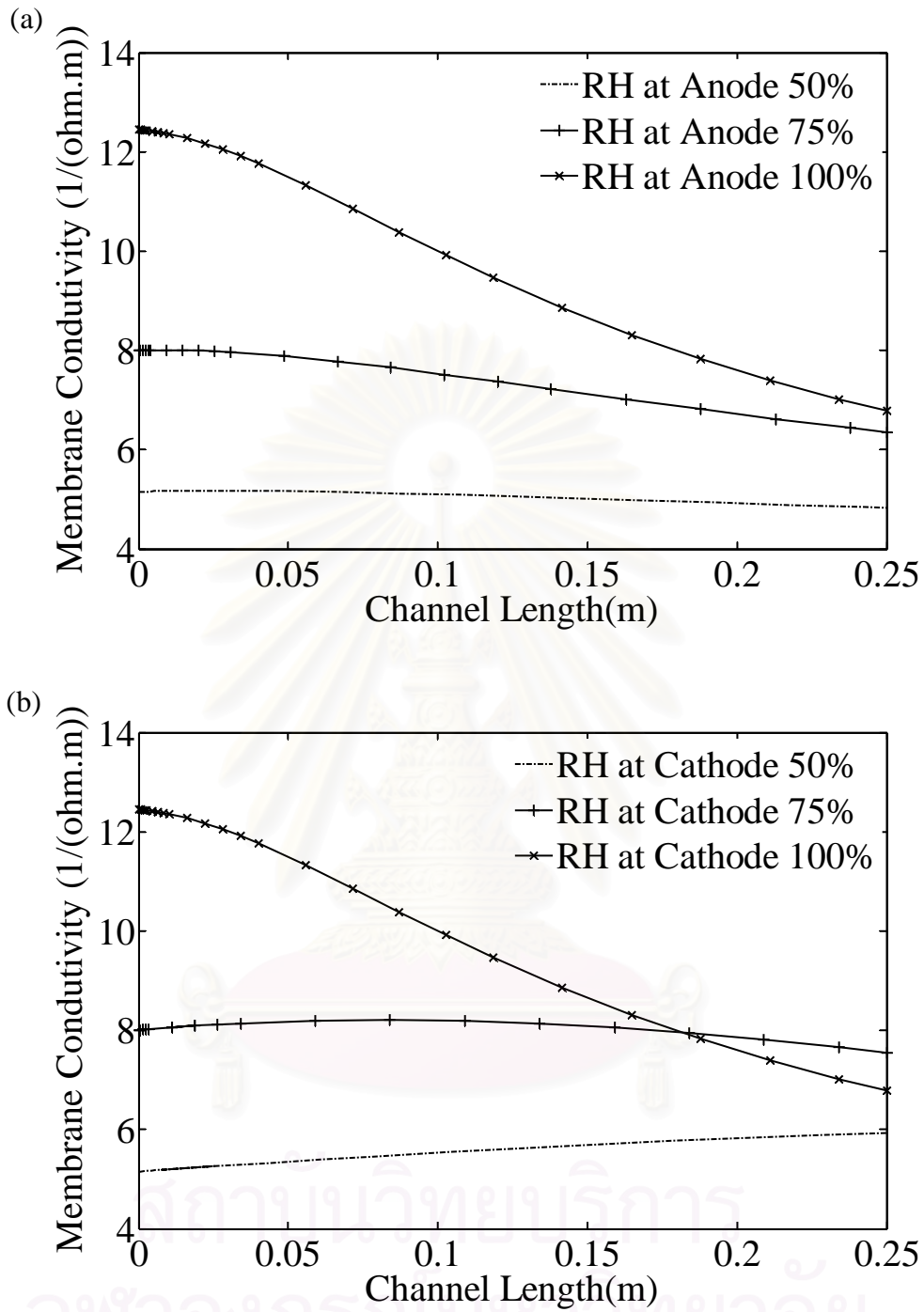


Figure 5.11 Distribution of membrane conductivity along the cell channel at different gas inlet humidity at (a) anode channel and (b) cathode channel.

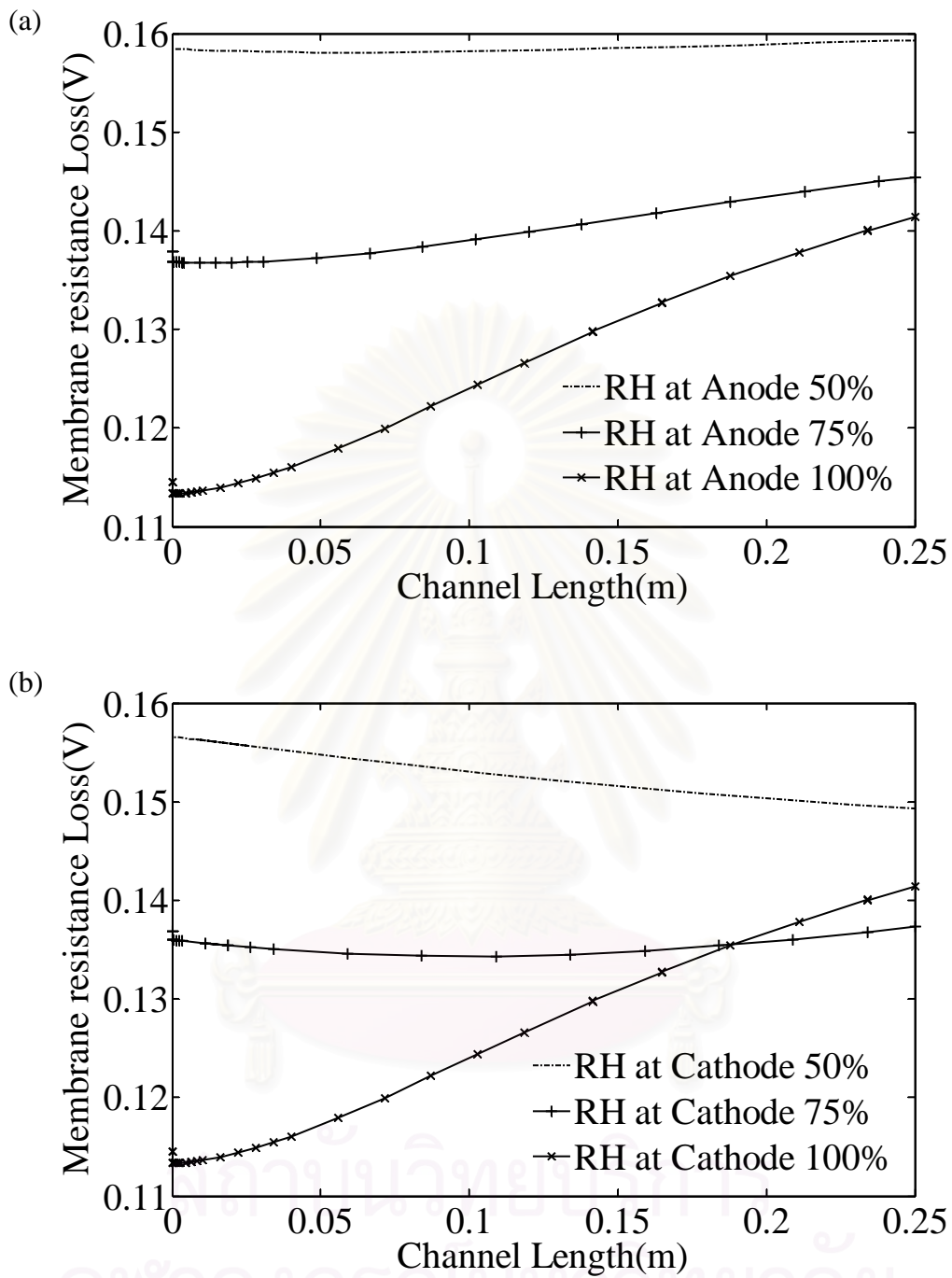


Figure 5.12 Distribution of membrane resistance along the cell channel at different gas inlet humidity at (a) anode channel and (b) cathode channel.

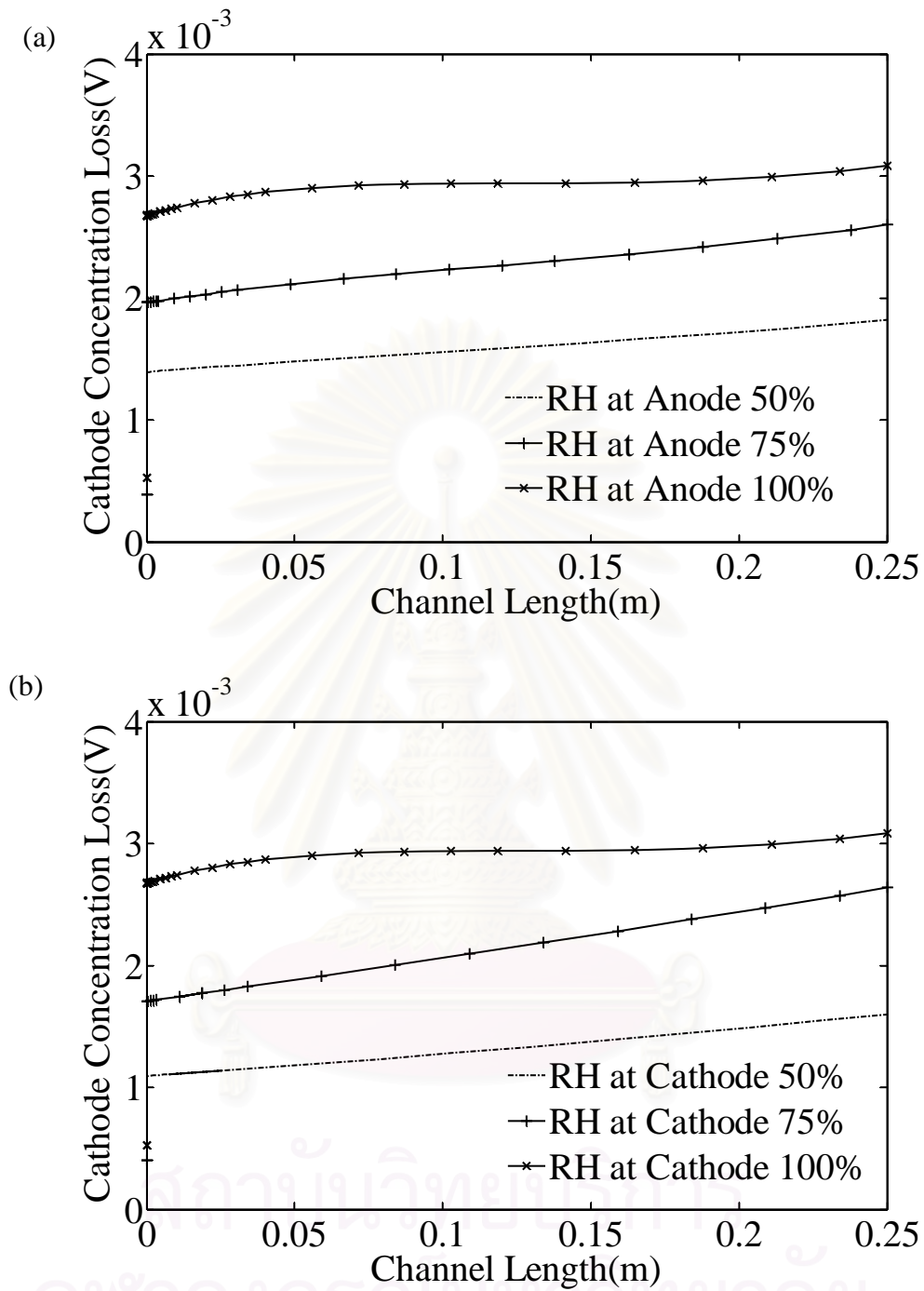


Figure 5.13 Distribution of concentration loss along the cell channel at different gas inlet humidity at (a) anode channel and (b) cathode channel.

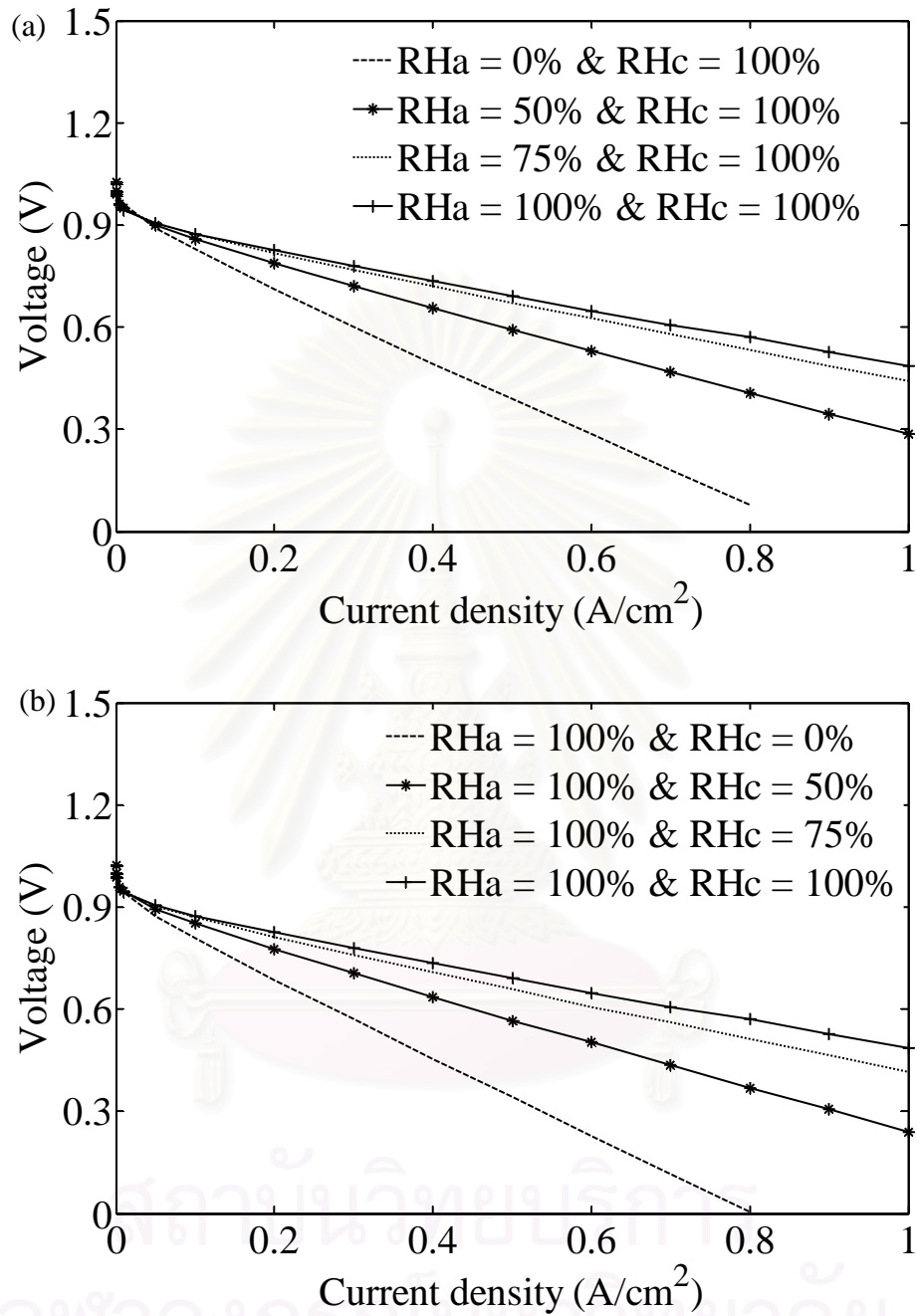


Figure 5.14 Effects of gas inlet humidity at different current density on cell voltage: (a) change of anode relative humidity, and (b) changing of cathode relative humidity.

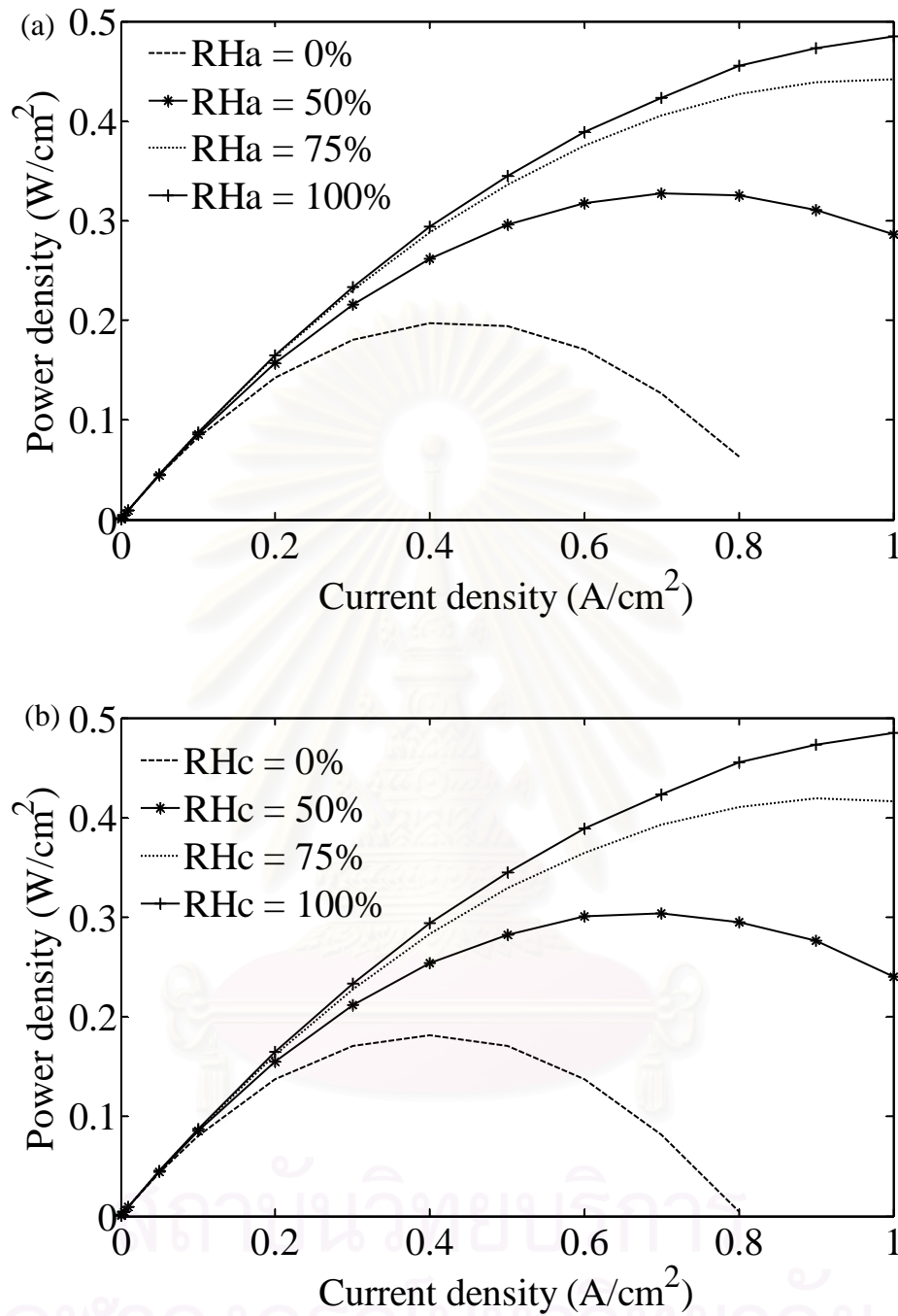


Figure 5.15 Effects of gas inlet humidity at different current density on cell power density: (a) change of anode relative humidity, and (b) changing of cathode relative humidity

The effect of the humidity of gas inlet at the anode and cathode channels on the polarization curve is further investigated. Figures 5.14(a) and 5.15(a) shows, respectively, the cell voltage and power density as a function of current density when the humidity of the fuel gas is varied from 0 % (dry gas) to 100 % and shown the humidity of the oxidant is fixed at 100% whereas Figures 5.14(b) and 5.15(b) shows, respectively, the cell voltage and power density at different current density when varying the humidity of the oxidant from 0 % to 100 %. It is found that increasing the humidity of the fuel gas leads to a significant improvement of cell performance. As the increased gas humidity causes more vapor water in the fuel, the membrane conductivity is increased and thus reducing the ohmic loss. Dry fuel gas dehydrated the membrane, so the cell performance is decreased rapidly. Figure 5.14 (b) shows that the humidified air also improve the cell performance. Although the dry air consists of high content of oxygen which can promote the electrochemical reaction, less vapor water in the air channel causes the membrane dehydrated, resulting in high ohmic overpotential. An increase of humidification of inlet air leads to the increased membrane conductivity and improved cell performance. From simulation results, it can be seen that the humidified fuel and air provides the improvement of the PEMFC performance.

5.5 Effect of anode inlet temperature

The effect of the anode inlet temperatures is studied in this section by changing the anode inlet temperature form 50 to 90 °C. The investigation of PEMFC performance is based on humidified inlet gas conditions. Figure 5.16(a)-(b) show the cell voltage and power density at different operating temperature and current density. It demonstrates that the cell voltage and power density decrease when the PEMFC is fed by fuel at higher temperature. An increase in fuel temperature at the inlet results in the dehydration of membrane. A decrease of hydrogen in fuel due to the increase of humidity temperature affect to the anode limiting current-density, especially at high current density. Thus, the PEMFC can be operated at low voltage and power density.

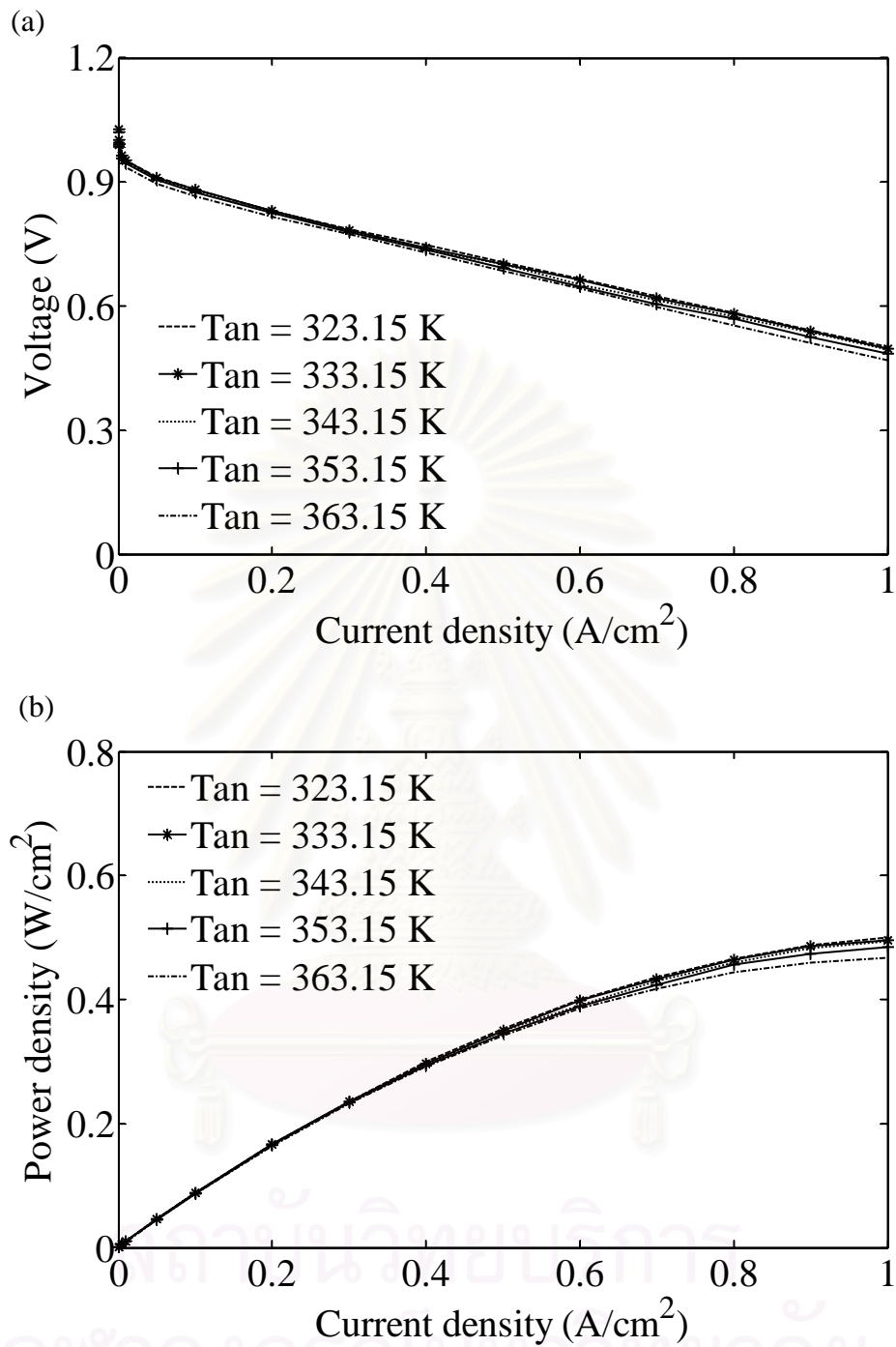
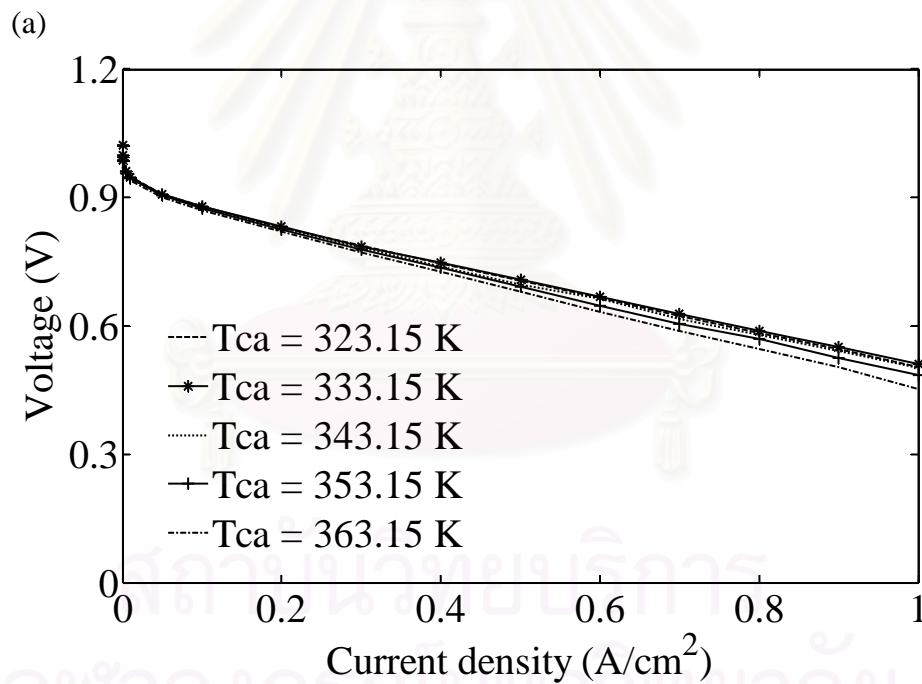


Figure 5.16 Effect of anode inlet temperature at different current density on (a) cell voltage and (b) power density.

5.6 Effect of cathode inlet temperature

The effect of the cathode inlet temperatures is analyzed by changing the cathode inlet temperature from 50 to 90 °C. The investigation of PEMFC performance is based on humidified inlet gas conditions. Figure 5.17(a),(b) show the cell voltage and power density at different operating temperature and current density. The results show that the cell voltage decreases while the cathode inlet temperature increases, especially at the high current density. This is because higher air inlet temperature results in the dehydration of membrane. In addition, a decrease of oxygen in air due to the increase of humidity temperature affects the limiting current-density which has an effect on cell voltage and power density.



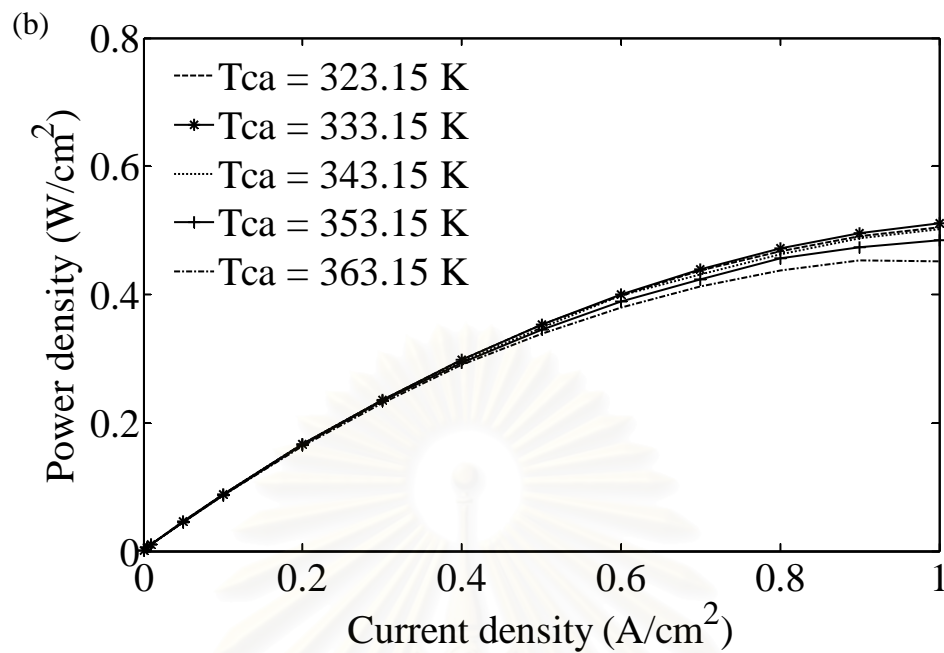


Figure 5.17 Effect of cathode inlet temperature at different current density on (a) cell voltage and (b) power density.

5.7 Effect of operating pressure

The effects of operating pressure at the anode and cathode sides on the characteristic curve are shown in Figure 5.18. The pressure is varied from 1 to 3 atm. It is found that the operating cell voltage slightly increases with increasing pressure. As the diffusivity of the reactant gases is increased, mass transport resistance decreases. Further, the increased operating pressure increases the partial pressure of reactants. This improves the PEMFC performance in terms of cell voltage and power density. However, increasing operating pressures decreases the water content of membrane that results in membrane dehydration and the increased ohmic loss.

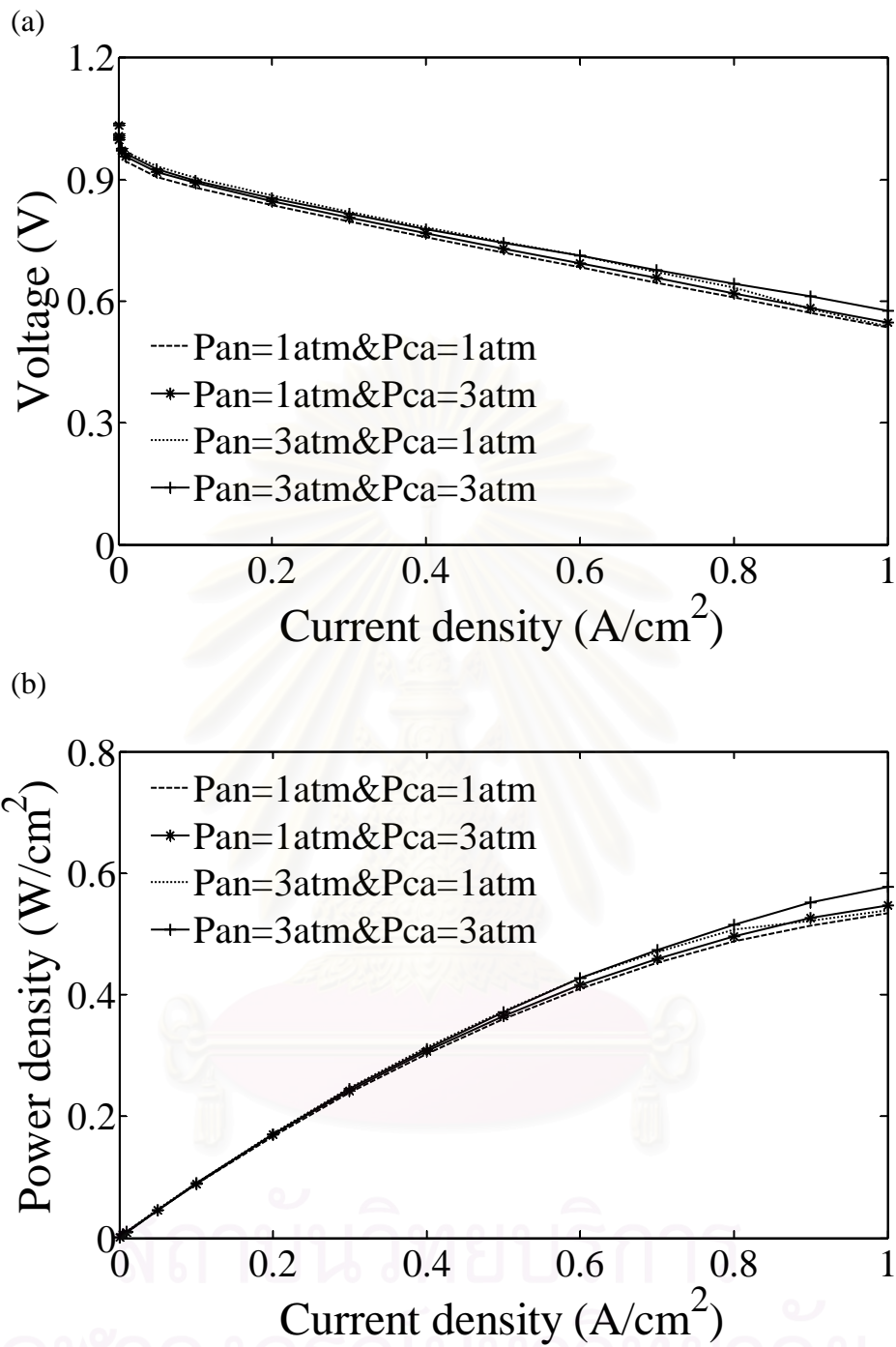


Figure 5.18 Effect of operating pressure at different current density on (a) cell voltage and (b) power density.

5.8 Effect of water flooding

Figure 5.19 shows the effect of operating current density on cell voltage and the fraction of water flooding when PEMFC is operated at 353 K and 1 atm and fed by humidified fuel and air. The results show that the fraction of water flooding at the cathode side increases with increasing operating current density. At high current density, more liquid water is produced and thus the fraction of water flooding increases. Increasing water flooding result in lower void fraction in the cathode and less oxygen can diffuse to the catalyst layer. Therefore, high concentration loss is observed. It is noted that the water flooding can be decreased by increasing volumetric flow rate of cathode gas to remove liquid water from the cell.

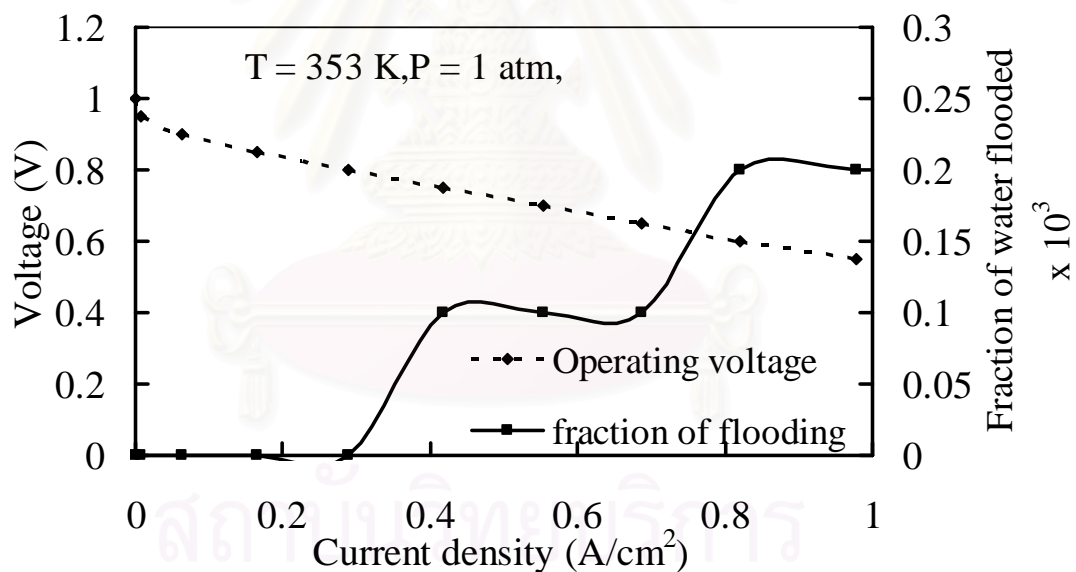


Figure 5.19 Effect of current density on cell voltage and fraction of water flooding.

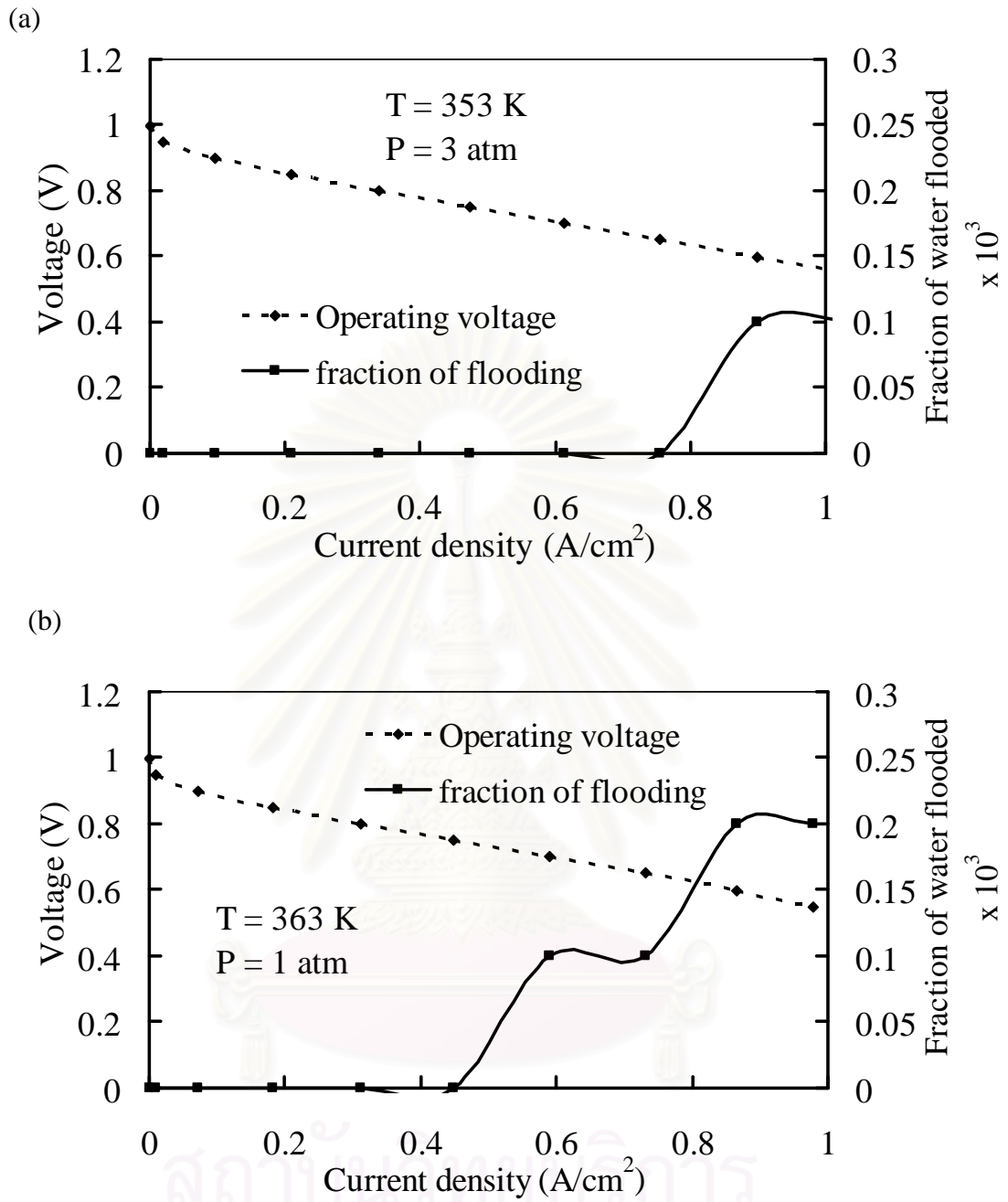


Figure 5.20 Effect of current density on cell voltage and fraction of water flooding at (a) $T = 353 \text{ K}$ and $P = 3 \text{ atm}$ and (b) $T = 363 \text{ K}$ and $P = 1 \text{ atm}$

Figure 5.20 shows the effect of operating current density on cell voltage and the fraction of water flooding at different operating pressure and temperature. It is found that when the PEMFC is operated at higher pressure and temperature, the occurrence of water flooding seems to be reduced. At low temperature, it make the cathode water vapor condense to liquid water because the cathode water vapor increases from electro-osmosis drag from anode to cathode and then the cathode partial pressure increase more than the saturated pressure at low temperature. It seems that the water flooding occurred earlier and increases rapidly at high current density. At high pressure, it makes the cathode activity decreases that result in the dehydration of membrane and then the liquid water evaporated because the cathode partial pressure decrease less than the saturated pressure.



สถาบันวิทยบริการ
จุฬาลงกรณ์มหาวิทยาลัย

CHAPTER VI

CONCLUSION AND RECOMMENDATION

6.1 Conclusion

This work studies on the simulation of polymer electrolyte membrane fuel cell (PEMFC) based on a two-phase steady state isothermal model. The mass transfer resistance of reactants due to water flooding is taken into account to analyze cell performance. Performance analysis of PEMFC in terms of the distribution of gas composition and current density, and cell voltage and power density is performed with respect to the effect of key operating conditions such as temperature, pressure and humidification of the reactant gases on the PEMFC.

Simulation shows that the cell performance increases with increasing operating temperature due to the decreased mass transport resistance and ohmic loss. Increasing the humidity of the fuel gas and air leads to a significant improvement of cell performance because an increase in high vapor water causes the membrane to have more water content and higher gas diffusivity and membrane conductivity. It is found that the cell voltage decreases while the anode and cathode inlet temperatures increase, especially at the high current density. This is because higher anode and cathode inlet temperature leads to the dehydration of membrane that causes high ohmic loss. Considering the influence of cell operating pressure, it is indicated that the increased pressure increases the partial pressure of reactants. This improves the PEMFC performance in terms of cell voltage and power density. By comparing with the result obtained from a single-phase PEMFC model in which water produced from the electrochemical reaction is in the vapor phase, it is found that the cell performance predicted by the two-phase model is lower than that obtained from the single phase model. Since the two-phase model accounts for the flooding effect on the gaseous reactant transport, an amount of oxygen permeated to the catalyst layer is lower. In addition, the liquid water causes higher ionic membrane resistances, thus leading to an increase in the ohmic loss.

Considering the effect of water flooding at the cathode, simulation results show that the occurrence of the water flooding increases with increasing operating current density. At high current density, more liquid water is produced and thus the fraction of water flooding increases. Increasing water flooding result in lower void fraction in the cathode and less oxygen can diffuse to the catalyst layer. Therefore, high concentration loss is observed. It is noted that the water flooding can be decreased by increasing volumetric flow rate of cathode gas to remove liquid water from the cell. The study of the electrical characteristics of PEMFC under the variation of key cell operating parameters contributes a useful tool for the understanding and improving of cell performance.

6.2 Recommendation

The performance of PEMFC is influenced by an operating temperature. The cell temperature is known to have an important impact on water management and transportation within the PEMFC. The future work should concentrate on the analysis of PEMFC under non-isothermal condition.

REFERENCES

- Barbir, F., PEM Fuel Cells Theory and Practice. Elsevier, London, 2005.
- Hayre, R.O., Cha, S.W., Colella, W., Prinz, F.B., Fuel Cell Fundamentals. John Wiley & Sons, New York, 2006.
- Amirinejad, M., Rowshanzamir, S. and Eikani, M.H., Effects of operating parameters on performance of a proton exchange membrane fuel cell. Journal of Power Sources 161 (2006): 872-875.
- Baschuk, J.J., and Li, X., Modeling of polymer electrolyte membrane fuel cells with variable degrees of water flooding. Journal of Power Sources 86 (2000):181-196.
- Bernardi, D.M. and Verbrugge, M.W., A mathematical model of the solid-polymer-electrolyte. Journal of Electrochemical Society 139 (1992): 2477-2490.
- Brett, D.J.L., Atkins, S., Brandon, N.P., Vasileiadis, N., Vesovic, V., and Kucernak A.R., Membrane Resistance and Current Distribution Measurements under Various Operating Conditions in a Polymer Electrolyte Fuel Cell. Journal of Power Sources (2007).
- Busquet, S., Hubert, C.E., Labbe, J., Mayer, D., and Metkemeijer, R., A new approach to empirical electrical modeling of a fuel cell, an electrolyser or a regenerative fuel cell. Journal of Power Sources 134 (2004): 41-48.
- Carnes, B. and Djilali, N., Systematic parameter estimation for PEM fuel cell models. Journal of Power Sources 144 (2005): 83-93.
- Chang, M., Chen, F., and Teng, H., Effects of two-phase transport in the cathode gas diffusion layer on the performance of a PEMFC. Journal of Power Sources (2006).
- Chen, K.I., Winnick, J., and Manousiouthakis, V.I., Global optimization of a simple mathematical model for a proton exchange membrane fuel cell. Journal of Computers & Chemical Engineering 30 (2006): 1226-1234.
- Costamagna, P., Transport phenomena in polymeric membrane fuel cells. Chemical Engineering Science 56 (2001): 323-332.
- Jeng, K.T., Lee, S.F., Tsai, G.F., and Wang, C.H., Oxygen mass transfer in PEM fuel cell gas diffusion layers. Journal of Power Sources 138 (2004): 41-50.

- Katsaounis, A., Tsampas, M., Balomenou, S.P., Tsiplakides, D., and Vayenas, C.G., Potential-dependent electrolyte resistance and steady-state multiplicities of PEM fuel cells. Journal of Solid State Ionics 177 (2006): 2397-2401.
- Lee, C. and Chu, H., Effects of cathode humidification on the gas-liquid interface location in a PEM fuel cell. Journal of Power Sources 161 (2006): 949-956.
- Lee, J.H., Lalk, T.R., and Appleby, A.J., Modeling electrochemical performance in large scale proton exchange membrane fuel cell stacks. Journal of Power Sources 70 (1998): 258-268.
- Liu, Z., Mao, Z., and Wang, C., A two dimensional partial flooding model for PEMFC. Journal of Power Sources (2005).
- Liu, Z., Mao, Z., Wang, C., Zhuge, W., and Zhang, Y., Numerical simulation of a mini PEMFC stack. Journal of Power Sources (2006).
- Mann, R. F., Amphlett, J. C., Hopper, M. A., Jensen, H. M., Peppley, B. A. and Roberge, P. R., Development and application of a generalized steady state electrochemical model for a PEM fuel cell, Journal of Power Sources 86 (2000): 173-180.
- Matamoros, L., and Bruggemann, D., Simulation of the water and heat management in proton exchange membrane fuel cells. Journal of Power Sources 161 (2006): 203-213.
- Meng H., A two-phase non-isothermal mixed-domain PEM fuel cell model and its application to two-dimensional simulations. Journal of Power Sources 168 (2007): 218-228.
- Mosdale, R., and Srinivasan, S., Analysis of performance and of water and thermal management in proton exchange membrane fuel cells. Journal of Electrochimica Acta 40 (1995): 413-421.
- Ramousse, J., Deseure, J., Lottin, O., Didierjean, S., and Maillet, D., Modeling of heat, mass and charge transfer in a PEMFC single cell. Journal of Power Sources 145 (2005): 416-427.
- Rowe, A., and Li, X., Mathematical modeling of proton exchange membrane fuel cells. Journal of Power Sources 102 (2001): 82-96.
- Santa Rosa, D.T.R., Pintoa, D.G., Silvaa, V.S., Silvab, R.A., and Rangel, C.M., High performance PEMFC stack with open-cathode at ambient pressure and temperature conditions. International Journal of Hydrogen Energy (2007).

- Santarelli, M.G., Torchio, M.F., and Cochis, P., Parameters estimation of a PEM fuel cell polarization curve and analysis of their behavior with temperature. Journal of Power Sources (2006).
- Shah, A.A., Kim, G.S., Gervais, W., Young, A., Promislow, K., Li, J., and Ye, S., The effects of water and microstructure on the performance of polymer electrolyte fuel cells. Journal of Power Sources (2006).
- Shimpalee, S., Dutta S.W., Lee, K., and Van Zee, J.W., Effect of humidity on PEM fuel cell performance Part II- Numerical simulation. Proceedings of ASME IMECE 364-1 (1999): 367 – 374.
- Siegel, N.P., Ellis, M.W., Nelson, D.J., Spakovsky, M.R., A two-dimensional computational model of a PEMFC with liquid water transport. Journal of Power Sources 128 (2004): 173–184.
- Singh, D., Lu, D.M., and Djilali, N., A two-dimensional analysis of mass transport in proton exchange membrane fuel cells. International Journal of Engineering Science 37 (1999): 431-452.
- Tsai, C.R., Chena, F., Ruoa, A.C., Chang, M.H., Chu, M.S., Soong, C.Y. , Yan, W.M., and Cheng, C.H., An analytical solution for transport of oxygen in cathode gas diffusion layer of PEMFC. Journal of Power Sources (2006).
- Um, S., and Wang, C., Computational study of water transport in proton exchange membrane fuel cells. Journal of Power Sources (2005).
- Wang, L., Husar, A., Zhou T., and Liu H., A parametric study of PEM fuel cell performances. International Journal of Hydrogen Energy 28 (2003): 1263 – 1272.



APPENDIX

สถาบันวิทยบริการ
จุฬาลงกรณ์มหาวิทยาลัย

APPENDIX A

LIST OF PUBLICATIONS

National conference

1. Worasorn Pothong, Yaneeporn Patcharavorachot, and Amornchai Arpornwichanop. Influences of Operating Variables on Polymer Electrolyte Membrane Fuel Cells. The 17th Thailand Chemical Engineering and Applied Chemistry Conference, Chiangmai, Thailand, Oct. 29-30, 2007: EFF17_1-3 (IN THAI).



สถาบันวิทยบริการ
จุฬาลงกรณ์มหาวิทยาลัย

VITA

Miss Worasorn Pothong was born in Phuket, Thailand on September 20, 1983. She received the Bachelor Degree in Chemical Engineering from Prince of Songkla University in 2006. After that she entered to Chulalongkorn University to pursue the Master of Engineering in Chemical Engineering and completed in 2008.



สถาบันวิทยบริการ
จุฬาลงกรณ์มหาวิทยาลัย